Title
A LIQUID PHASE DENSIFICATION TECHNIQUE FOR THE LEAD ZIRCONATE TITANATE SYSTEM

Author
Sherohman, John W.

Publication Date
1974-11-01

A LIQUID PHASE DENSIFICATION TECHNIQUE FOR THE LEAD ZIRCONATE TITANATE SYSTEM

John W. Sherohman, Jr.
(Ph. D. Thesis)

November 1974

Prepared for the U. S. Atomic Energy Commission
under Contract W-7405-ENG-48

DISCLAIMER

Table of Contents

A LIQUID PHASE DENSIFICATION TECHNIQUE FOR THE LEAD ZIRCONATE TITANATE SYSTEM

John W. Sherohman, Jr.

Inorganic Materials Research Division, Lawrence Berkeley Laboratory, and Department of Materials Science and Engineering, College of Engineering; University of California, Berkeley, California 94720

ABSTRACT

By combining conventional processing methods that are known to enhance sintering, a unique liquid phase densification technique has been investigated for the PZT system. The technique is a two-step process: (1) utilization of a low temperature liquid phase ($PbO \cdot PbF_2$) to optimize, with the aid of applied pressure, the rearrangement of the PZT particles on formation of the liquid, and (2) a subsequent heat treatment to allow liquid phase sintering to occur. During this heat treatment a fixed PbO atmosphere was established to remove the liquid from the PZT material in a controlled manner, thus producing a dense single phase PZT ceramic of fixed stoichiometry.

The evaporation of $PbO \cdot PbF_2$ from $PZ_{.5}T_{.5}$ was experimentally observed using thermogravimetry. The evaporation rate was found to be dependent on the partial pressure of PbO as set by multi-phase packing powder compositions within the PZT system. The rate of liquid removal was further sensitive to both the density and temperature of the $PZ_{.5}T_{.5}$ specimen. As the density increases to a closed pore geometry, the rate of evaporation of the liquid phase became thickness dependent. The PbO vapor pressure of the $PZ_{.5}T_{.5}$ material containing the PbO rich liquid was determined for the evaporation rate in a PT + P packing powder using the Langmuir equation. By comparing the Langmuir PbO vapor pressure at

different temperatures with the PbO vapor pressure from Knudsen effusion data, the evaporation coefficient was calculated as approximately 1.8 x 10^{-6} in the temperature range of 1150° to 1250°C. In addition, ferroelectric and piezoelectric measurements were made on $PZ_{.5}T_{.5}$ specimens of various intrinsic nonstoichiometry that were initially densified by the liquid phase densification technique.

I. INTRODUCTION

Because of the ferroelectric nature of the lead zirconate titanate (PZT) system, it has been utilized for many years in the fabrication of piezoelectric devices. It is favored for these devices because of its large piezoelectric effects, high Curie temperature, and high permittivity. Along with these properties, the PZT system has the ability to function within a wide range of ferroelectric and piezoelectric applications by intentional variation of the ratio of zirconium to titanium, or by partial replacement of lead, titanium, or zirconium by other elements.[1-6] Yet its ferroelectric and piezoelectric parameters are not only affected by composition, but are further sensitive to variations in density and grain size.[7-9] Also, it has been shown that electro-optic devices can be made from modified PZT compositions. Lanthanum modified lead zirconate titanate (PLZT) is optically transparent when near theoretical density and has the ability to behave as an electrically controlled light scatterer or retarder depending on the grain size.[10-14] Chemical composition and microstructure are therefore important factors that can determine functional usage.

In addition, changes in chemical composition due to nonstoichiometric effects must be controlled to maintain the PZT composition in its single phase region. Because there exists a high vapor pressure of lead oxide (PbO) at temperatures required for densifying PZT powder compacts, an intrinsic nonstoichiometric composition can occur.[15-18] If the evaporation of PbO from the PZT ceramic is not controlled, loss of PbO can lead to the development of second phases (e.g. ZrO_2 and TiO_2). It has been shown that loss of PbO from the system can affect both the

electrical and physical properties.[19-21]

Variation in stoichiometry during densification of PZT must therefore be controlled along with development of a desirable microstructure to produce reproducible and predictable ceramics. Although densification of the PZT system has been achieved by both hot pressing and normal sintering techniques, both processing schemes require many hours at relatively high temperatures. Consequently, difficulties exist in maintaining a fixed stoichiometry during processing. In the case of unmodified PZT, it is difficult to obtain densities higher than 95% of theoretical.

High relative density can generally be obtained in the PZT system when the addition of a dopant affects the grain growth behavior by solid solution substitution in the lattice. The dopant acts as a grain growth inhibitor that allows the pores to remain on the grain boundaries where pore elimination can take place by grain boundary diffusion. Without a grain growth inhibitor, exaggerated grain growth may occur that can lead to entrapment of pores within the grains and produce a density limitation; removal of the pores, in this case by bulk diffusion of lattice vacancies, would require comparatively long times. Even though use of a dopant may result in a highly dense PZT and give control over grain growth, the composition has been modified. Since the ferroelectric and piezoelectric properties are dependent on chemical composition and microstructure, the need of a dopant prevents the determination of the intrinsic electrical properties of PZT. A processing scheme is therefore of importance that can establish a controlled PbO atmosphere to maintain stoichiometry and achieve high density (even in unmodified PZT) without affecting the initial composition.

The purpose of this study was to employ a combination of processing methods to investigate a unique densification technique that can achieve a highly dense, unmodified single phase PZT ceramic with fixed stoichiometry. To develop a processing procedure to improve the densification and quality of unmodified PZT, a review of the conventional processing techniques was necessary.

A. Sintering PZT

Sintering is often referred to as a process whereby powder particle compacts are heat treated to achieve densification by removal of porosity. This process occurs due to the decrease in the surface free energy associated with the decrease of surface area during densification. Material transport mechanisms that have been generally accepted to lead to pore removal in oxide ceramics are volume diffusion and viscous or plastic flow. However, a viscous or plastic flow mass transport mechanism has not been experimentally verified as applicable to the sintering of ceramics except in the initial stages of sintering glass spheres.[22] As a consequence, material transport by a diffusion controlled process has been the accepted mechanism for solid state sintering.

1. Sintering Aid

Coble[23,24] has developed a model to describe the intermediate and final stages of sintering based on diffusion of lattice vacancies from pores to grain boundaries. Atkin and Fulrath[21] have shown that unmodified PZT behaves according to the kinetics predicted by the Coble model, but that it is difficult to obtain a highly dense PZT ceramic unless a sintering aid is utilized. The addition of an impurity generally aids in sintering by preventing exaggerated grain growth from occurring. Reducing

grain boundary mobility and, therefore, grain growth is important since solid state sintering involves many hours at relatively high temperatures to achieve a dense ceramic.

Although an impurity can aid in control of the microstructure, it also has an effect on the PZT electrical properties. Depending on the atomic radii of the impurity atom along with its valence, its presence in the lattice influences the ferroelectric and piezoelectric properties.[21,25] Because the ferroelectric and piezoelectric behavior are dependent on both composition and microstructure, the true intrinsic electrical properties have not been measured on highly dense unmodified PZT.

2. Lead Oxide Atmosphere

Since the sintering of PZT requires relatively high temperatures to achieve densification, the loss of PbO from the system must be prevented.* Loss of PbO results in intrinsic nonstoichiometric changes in composition that can lead to the development of second phases. An advantage of the sintering process is that during the heat treatment the PZT samples can be placed in an environment of a packing powder of PZT composition to buffer the loss of PbO from the samples. Variations of this technique have been used to reduce PbO evaporation.[2,26,27] Only recently have studies been concerned with the PbO vapor pressure above the PZT system.[21,28-30] Atkin and Fulrath[21] have shown the densification and grain growth behavior of both modified and unmodified PZT sintered in

*Loss of TiO_2 or ZrO_2 from the system is insignificant since their vapor pressures are negligible at the temperatures required for sintering PZT.

atmospheres of various PbO and oxygen activities. Holman and Fulrath[29] have shown that by establishing the correct PbO activity, the single phase width of a PZT composition can be determined with temperature. Experimental results have thus indicated that the evaporation of PbO from the sample can be controlled by heat treating in a fixed PbO atmosphere.

B. Pressure Sintering

1. Densification Mechanisms

Removal of porosity by sintering under the influence of an external pressure is a densification process known as hot pressing or pressure sintering. Pressure is applied to a powder compact by means of a die assembly that can withstand both pressures and temperatures required to promote densification. With the aid of applied pressure, an increase in the rate of densification of the sample can result because of mechanisms not found in the normal sintering process.

Pressure sintering densification mechanisms that have been suggested to explain an increase in the rate of densification under stress are particle rearrangement (occurs particularly during early stages of compaction), plastic flow, and stress enhanced diffusion models. Of these mechanisms, particle rearrangement and stress enhanced diffusion have been proposed by Haertling[31] to explain the densification behavior of hot-pressed modified PZT. Comparison of the densification rate of PZT under different stresses indicated a linear relationship and was accounted for by a Nabarro-Herring mechanism of stress directed movement of vacancies. Based on a low activation energy value as determined from an Arrhenius plot of diffusion coefficients calculated from the Nabarro-

Herring equation, Haertling further suggested that viscous behavior due to grain boundary sliding was also contributing to the densification process. Hence, experimental evidence tends to indicate that particle rearrangement appears to be an important mechanism in the initial densification of hot-pressed PZT.

2. Controlled Microstructure

Since pressure sintering introduces densification mechanisms that can increase the rate of densification as compared to that of the normal sintering process, it offers a method of acquiring control of the microstructure. By the use of external pressure, a highly dense sample can generally be obtained at lower temperatures and in less time than in pressureless sintering. The density of the sample can often be established before appreciable grain growth occurs. The desired grain size can then be developed by a subsequent isothermal heat treatment. Control of the microstructure by this approach has been performed on modified PZT to demonstrate the effects of microstructure on its electrical properties. Okazaki and Nagata[7,8,11] have produced modified PZT samples with constant grain size and variable density along with samples of constant density and variable grain size by a hot-pressing technique.

3. Loss of Lead Oxide

Although hot pressing is a processing method that can lead to a controlled microstructure, the lack of control of the loss of PbO from the PZT sample remains a problem. With external pressure, the rate of densification is enhanced, allowing densification to proceed at lower temperatures; yet temperatures above 1000°C are generally necessary to develop a fully dense modified PZT sample. Vapor pressures of PbO above

the PZT system as determined by Knudsen effusion experiments indicate that the vapor pressure of PbO is significant even at temperatures of 1000°C.* Development of an intrinsic nonstoichiometric PZT from the loss of PbO can therefore occur during hot pressing.

C. Liquid Phase Sintering PZT

Sintering in the presence of a liquid phase is a processing technique that often leads to enhanced densification. The technique is similar to that of normal sintering in that a compact of powder particles is heat treated to achieve densification without applied pressure. The difference lies in the intentional addition to the compact of a second phase material that forms a liquid during the heat treatment. Kingery[32] has outlined the requirements for liquid phase sintering to be effective in obtaining complete densification. It is essential to have (1) an appreciable amount of liquid phase, (2) an appreciable solubility of the solid in the liquid, and (3) complete wetting of the solid by the liquid for rapid liquid phase densification.

On formation of the liquid phase, the initial rapid increase in density is attributed to the rearrangement of the solid particles due to liquid flow. Further densification of the compact proceeds by an increase in the solubility at the solid-liquid interface between solid particles because of capillary compressive forces.[33] In this way, densification can take place since precipitation away from the contact area by transfer of material through the liquid allows the decrease of the center-

---

*The vapor pressure of PbO above $Pb(Zr_{.5}Ti_{.5})O_3 + ZrO_2 + TiO_2$ is approximately 10^{-5} atm at 1000°C.[30] As a result, the PbO vapor pressure above single phase $PZ_{.5}T_{.5}$ is sufficient to develop multiphases.

to-center distance between the particles.

Although sintering with an appropriate liquid can increase the rate of densification, the liquid phase is generally retained in the microstructure. Consequently, this result is usually detrimental in applications requiring ceramics as insulators. If the dielectric constant of the crystallized liquid phase is much lower than that of the solid, dielectric breakdown will often occur through the second phase at relatively lower electric fields. Because the dielectric constant of PZT is rather high (1100 as measured at 100 Hz[6]), the presence of a second phase between the grains is undesirable. Atkin[34] has shown that the ferroelectric properties of PZT can be altered by silica additions where a silicate glass liquid phase covered each of the ferroelectric grains and served as a series capacitance.

Use of excess PbO in the PZT system to form a lead oxide rich liquid phase has been attempted by Brown and Mazdiyasni[35] and Snow[27,36] in sintering chemically prepared PLZT. Their results showed that a PLZT material of optical transparency comparable to that obtained by hot pressing can be fabricated by liquid phase sintering. Brown and Mazdiyasni sintered PLZT that was synthesized from metal alkoxides and achieved complete densification in eight hours at 1120°C. Their samples contained 10 wt% excess PbO and were fired in a packing powder of the same composition as the sample. Snow acquired complete densification of PLZT prepared from metal alkoxides, with the exception of the lead addition,* only after sintering for 60 hours at 1200°C. His samples

*A lead oxide powder was used instead of an alkoxide of lead.

contained approximately 6.6 wt% excess PbO and were heat treated in an alumina crucible arrangement that contained either a $PbZrO_3$ or a $PbZrO_3$ + PbO_2 packing powder composition. The difference in the processing parameters to obtain optical transparent PLZT suggest the importance of studying the behavior of the liquid phase during sintering. The optimum amount of excess PbO and the ability to control the removal of the liquid phase are necessary factors that need to be investigated.

D. Combination of Techniques

In both the hot pressing and liquid phase sintering techniques, the rate of densification is enhanced as compared to normal sintering. But with the problem of PbO evaporation in PZT and the possible detrimental effect of second phases on the electrical properties, these techniques alone are not optimum processing methods to control intrinsic non-stoichiometry. By using a combination of these techniques for rapid densification and an understanding of how to properly control the loss of PbO from the system, a unique liquid phase densification technique has been investigated to develop a highly dense unmodified single phase PZT ceramic with fixed stoichiometry.

The procedure for this technique is essentially a two-step process. The first step makes use of a low temperature liquid phase that can optimize, with the aid of external applied pressure, the rearrangement process on formation of the liquid. The second step involves a subsequent heat treatment without applied pressure to allow liquid phase sintering to occur. During this heat treatment, a fixed PbO atmosphere is established that permits the liquid to be removed in a controlled manner and maintain the PZT sample within its single phase region.

II. EXPERIMENTAL

A. Powder Preparation

For the purpose of comparison, a PZT composition of $Pb(Zr_{.5}Ti_{.5})O_3$, which will be written as $PZ_{.5}T_{.5}$, was prepared from both mixed oxides and chemical compounds. Appropriate amounts of lead oxide,* zirconium dioxide,** and titanium dioxide† powders were used to form the mixed oxides composition. In the case of the chemically prepared powder, the $PZ_{.5}T_{.5}$ composition was made from an initial solution containing proper amounts of lead oxide powder,* zirconium tetra-n-butoxide liquid ($Zr(OBu)_4$),†† titanium tetra-n-butoxide liquid ($Ti(OBu)_4$),†† along with isopropyl alcohol and distilled water. The low temperature liquid phase added to both powder preparations after forming $PZ_{.5}T_{.5}$ was a lead oxyfluoride ($PbO{\cdot}PbF_2$) composition that has a melting temperature of approximately 500°C. A flow chart outlining the procedure in the preparation of the mixed oxides, the chemically prepared, and the lead oxyfluoride powders is shown in Fig. 1.

A calcining temperature of 1200°C was used in the powder preparation of the mixed oxides to insure complete reaction. An isostatic pressed slug of the mixed oxides was fired in a platinum crucible at 1200°C for five hours in a PZ+Z packing powder to buffer the loss of PbO. The powder preparation used for the chemically prepared material essentially follows the procedure outlined by Haertling and Land[37] in the preparation of chemically prepared PLZT. Both thermogravimetric analysis (TG) and

---

* Baker, reagent grade.
** Wah Chang, reactor grade.
† B & A, reagent grade.
†† Dynamit Nobel of America, Northvale, New Jersey.

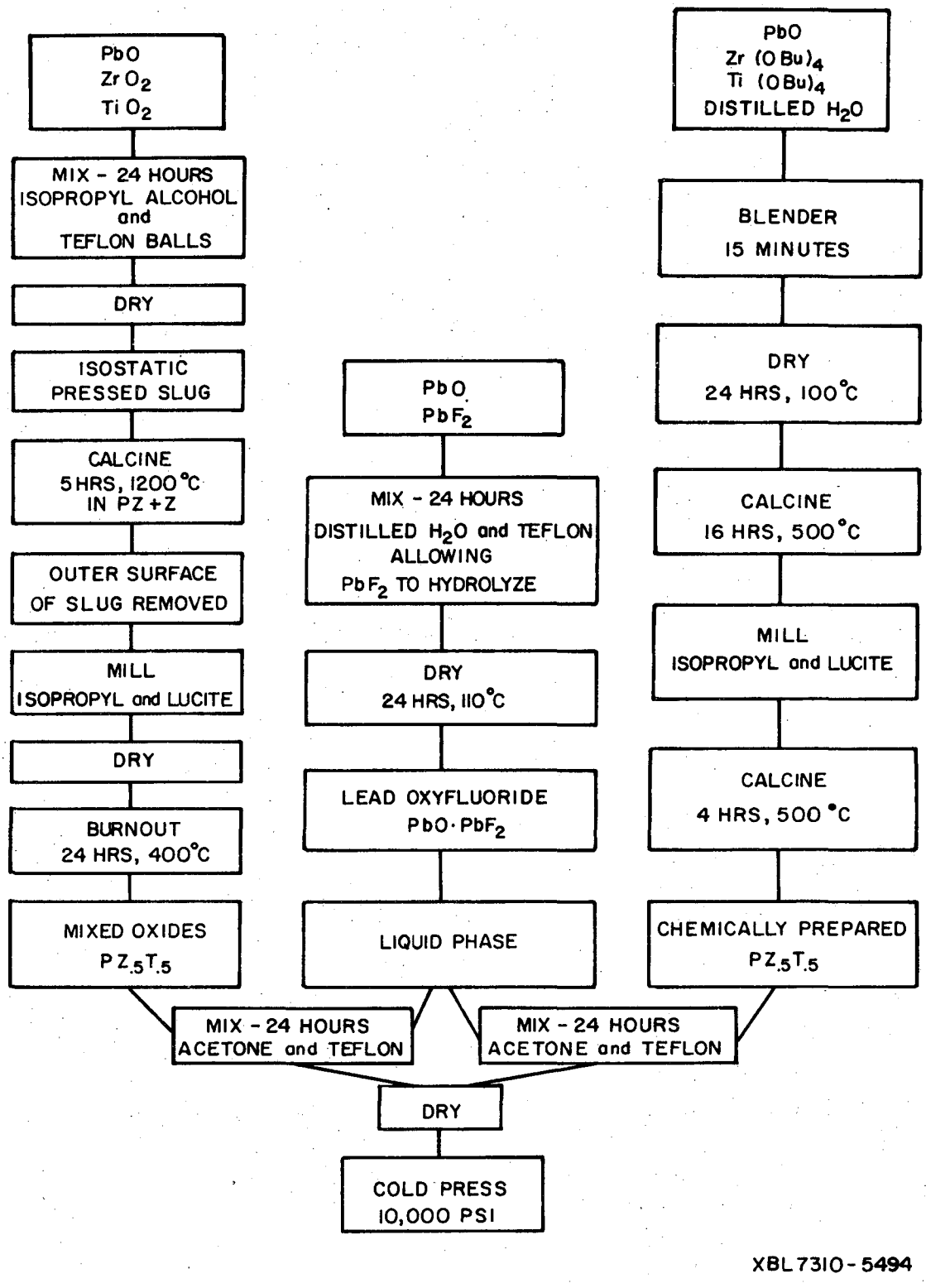

Fig. 1. Powder preparation flow chart for the mixed oxides, the chemically prepared, and the liquid phase materials.

differential thermal analysis (DTA) were performed on the chemically prepared powder for purposes of characterization. A semiquantitative spectrographic analysis* of the impurity content of the $PZ_{.5}T_{.5}$ and the lead oxyfluoride materials is given in Table I. The specific surface area of the materials was also determined by a one-point BET method using a Perkin-Elmer sorptometer.

B. Hot-Pressing Process

To determine the proper liquid content to obtain maximum density in the first step of the process, various weight percents of the "liquid" phase were mixed with both the mixed oxides and chemically prepared PZT powder. The mixed material was cold pressed at 10,000 psi in a 3.2 cm diameter die to form an initial compact that was then placed in a stainless steel hot-press die assembly shown in Fig. 2. A 3.5 cm diameter stainless steel insert was used to allow movement of the course (-36 + 80 mesh) zirconia sand into the free volume and provide a better transfer of force to the powder compact. A pre-load of 1000 lbs was applied to the die while heating in helium to 600°C at a rate of 10°C per minute. On reaching temperature, a load of 12,000 lbs was applied to the die for 3.5 hours and displacement of the sample was monitored by a Linear Variable Differential Transformer. After hot pressing, the die was immediately removed from the press and allowed to air cool. The pressed sample was then taken out of the die and its outer layer ground away to remove zirconia particles that were embedded in the surface.

---

* American Spectrographic Laboratories

TABLE I

Impurity* Element	Mixed Oxides $Pb(Zr_{.5}Ti_{.5})O_3$	Chemically Prepared $Pb(Zr_{.5}Ti_{.5})O_3$	Lead Oxyfluoride ($PbO \cdot PbF_2$)
Hf	-	.5%	-
Si	.005%	.01	<.005%
Bi	.025	.025	.015
Al	.06	.02	<.001
Cu	.007	.003	<.001
Ni	.015	.02	-
Ba	<.001	<.001	-
B	-	.005	-
Mg	.001	-	<.001
Fe	-	-	.005
Ag	-	-	<.001
Co	.002	.002	-
Ca	.02	-	.002

*Reported as weight percent of the oxides of the elements.

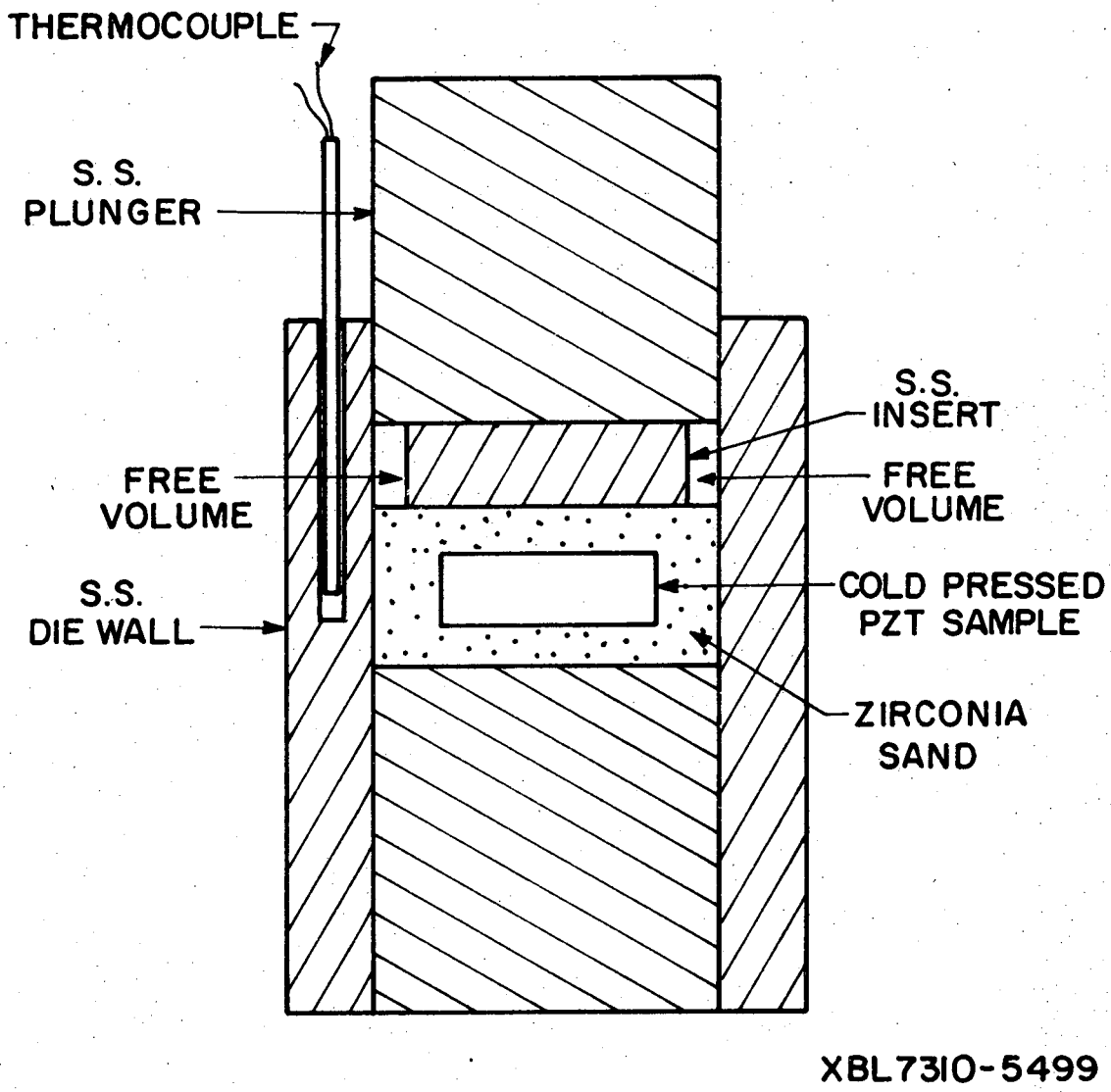

Fig. 2. Stainless steel hot-press die assembly.

The amount of liquid phase remaining in the sample after pressing was determined by recording the sample weight loss by TG. This was accomplished by slicing a 0.8 mm thick rectangular plate from the pressed sample on an Isomet diamond saw and placing the specimen in a platinum wire cage that was attached to a R-100 Cahn balance. The sample was heated rapidly to 1000°C in air by a platinum wound furnace and the weight loss was recorded. After removal of the liquid as determined by the rate of weight loss at 1000°C, the sample was immediately air cooled and the density was measured and compared to the density obtained in other pressed samples of various liquid content. The highest density specimen indicated the weight percent liquid phase addition necessary to optimize the first step in the liquid phase densification technique. This procedure was performed for both the mixed oxides and chemically prepared $PZ_{.5}T_{.5}$ compositions.

C. Liquid Phase Sintering Process

1. Mixed Oxides Material

After establishing the proper amount of liquid content for the initial hot-pressing step, a study of removing the liquid from the pressed sample in a controlled manner during liquid phase sintering was investigated. Specimens of rectangular shape of approximately 5 mm wide and 10 mm in length were obtained from a mixed oxide hot-pressed sample and ground with 600 mesh SiC powder to achieve both a 0.8 mm and 1.6 mm thickness. A specimen of each thickness was packed in different multi-phase powder compositions within the PZT system in a platinum crucible and heated in O_2 at a rate of 86°C/hr to 1200°C. The packing powder compositions were chosen to establish atmospheres of various PbO

activities that would allow the sample to equilibrate by losing PbO, but still maintain the sample in its single phase region. The specimens were held at temperature for different time intervals in the packing powder compositions of lead zirconate plus 5 wt% zirconia (PZ+Z), lead titanate plus 5 wt% PbO (PT+P), and $PZ_{.5}T_{.5}$ plus 5 wt% PbO ($PZ_{.5}T_{.5}$+P). After the heat treatment, the specimens were rapidly cooled to room temperature.

The amount of liquid remaining in the specimens as a result of firing in different PbO atmospheres for various times at 1200°C was determined by thermogravimetry. The specimens were reheated rapidly to 1000°C (in an attempt to reduce additional liquid phase sintering) and the weight loss of the specimens was monitored by the R-100 Cahn balance. The fraction of liquid removed from the sample was calculated by comparing the amount of weight loss after liquid phase sintering to the total weight loss after hot pressing. After removal of the liquid by evaporation, the density of the specimens was measured by immersion in distilled water.

2. Chemically Prepared Material

A hot-pressed chemically prepared sample containing the optimum amount of liquid phase, as determined by the first step in the process, was used for a liquid phase sintering study. Rectangular shape specimens of 1.8 mm thick, 3 mm wide, and 10 mm in length were heat treated by using a double platinum crucible geometry as shown in Fig. 3. A thin layer of coarse (-36 +80 mesh) zirconia setting sand was used to separate the specimen from the inner crucible. Use of the double crucible allowed removal of the liquid phase from the specimen through the vapor phase,

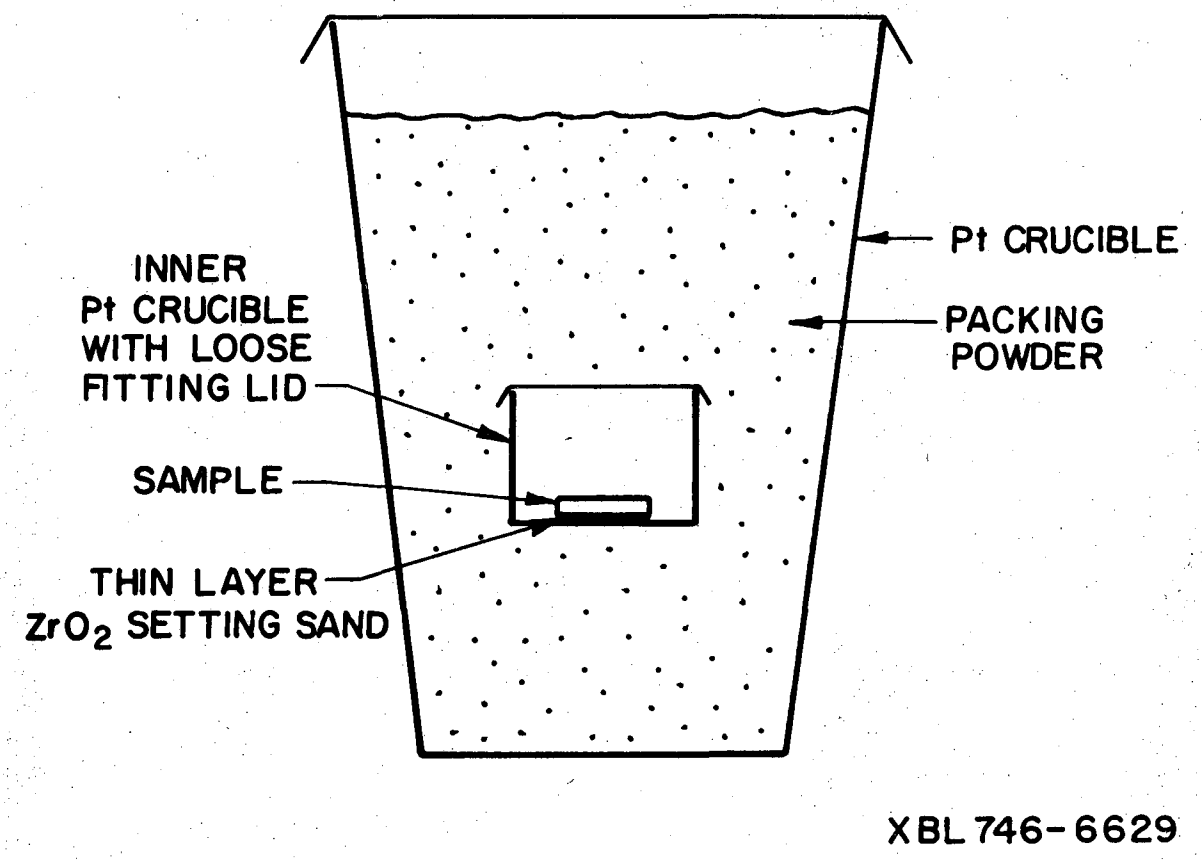

Fig. 3. Double platinum crucible for heat treatment of the chemically prepared $PZ_{.5}T_{.5}$.

avoiding direct contact with the liquid phase in the packing powder.

The specimens were heated in O_2 at a rate of 86°C/hr and held for one minute at temperatures in the range from 1000° to 1200°C in a packing powder of PT + P. After removal of the remaining liquid by thermogravimetry at 1000°C in air, the fraction of liquid removed, the densities, and the grain sizes were measured. The grain size was determined by the line intercept method[38] from photomicrographs of polished surfaces that were chemically etched by a 5% HCl solution containing several drops of 48% HF. The densities were obtained by immersion of the specimens in distilled water.

D. Temperature Dependence

The effect of temperature on liquid phase removal was investigated by firing 0.8 mm thick mixed oxide specimens in a packing powder of PT + P. The specimens were heated at a rate of 86°C/hr in O_2 to a temperature in the range of 1050° to 1250°C and held for successive intervals of time extending up to 12 hours. After holding at temperature for the different time intervals, the specimens were rapidly cooled to ambient temperature. The fraction of liquid removed, the density, and the grain size of the specimen were determined. The grain sizes were determined by the line intercept method from photomicrographs of polished surfaces that had been etched.

From the fraction of liquid removed, the rate of weight loss from the specimens in a PT + P packing powder composition was determined at various temperatures. Because the rate of weight loss is a measure of the rate of escape of molecules from the surface of the specimen, the weight loss behavior was correlated to a Langmuir method for measuring

vapor pressures. Assuming the Langmuir postulate that the number of molecules leaving a surface is independent of the number of gas molecules striking the surface, the Langmuir equation was used to calculate the vapor pressure at different temperatures. By comparing the Langmuir vapor pressure to the vapor pressure determined by Knudsen effusion experiments,[30] the evaporation coefficient was obtained for liquid phase evaporation from $PZ_{.5}T_{.5}$ in a PT+P packing powder. Also, by plotting the Langmuir vapor pressure along with the vapor pressure from Knudsen effusion data versus reciprocal temperature, a comparison was made of the apparent enthalpy and entropy for evaporation of the liquid phase.

E. Ferroelectric and Piezoelectric Measurements

The ferroelectric and piezoelectric behavior of $PZ_{.5}T_{.5}$ was investigated by firing samples in different packing powder compositions having a PbO activity that allowed the intrinsic nonstoichiometry of the samples to remain within the single phase region. Specimens of $PZ_{.5}T_{.5}$ prepared from mixed oxides were sintered by the liquid phase densification technique. Each specimen was initially ground to approximately 0.8 mm thickness and heated in O_2 at a rate of 86°C/hr to a temperature of 1250°C in the double platinum crucible geometry. The specimens were held at temperature for eight hours and the liquid phase was removed in an atmosphere of PbO set by a PT+P packing powder composition. After the heat treatment, the specimens were furnace cooled and then further ground to a thickness of approximately 0.4 mm using 1000 mesh SiC powder.

The specimens were once again placed in the double platinum crucible geometry with the exception that this time each was surrounded by a different multi-phase packing powder composition. A heat treatment of

1100°C in air was performed for 24 hours to allow the specimens to equilibrate with the packing powder composition whose PbO activity permitted the specimens to remain within their single phase region. After the specimens had furnace cooled, they were prepared for both ferroelectric and piezoelectric measurements.

The specimens were diamond-core drilled to form disks of 4 mm in diameter and air drying electrodes were applied using a silver conducting paint.* Ferroelectric parameters were determined from P-E hysteresis loops using a Sawyer-Tower circuit by applying an effective voltage of 900V at 60 Hz. The coercive electric field, E_c, the remanent polarization, P_r, and the maximum polarization,** P_m, were measured.

Similar disks were electrically poled in silicone oil using a DC field of 15 KV/cm. After the poled disks had aged for 24 hours, the dielectric constants were determined from a General Radio impedance bridge type 1650-A at 1 KHz. In addition, the resonant and antiresonant frequencies, f_r and f_a, of the disks were obtained and the planar coupling factor, k_p, and the piezoelectric constant, d_{31}, were calculated. By a direct measurement of displacement, X, of the disks versus a small applied electric field, the planar piezoelectric constant, d_p, was determined from the slope of X versus E as recorded on an X-Y plotter.

---

* Micro-Circuits Co.
** Measured at maximum electric field.

III. RESULTS AND DISCUSSION

To investigate a processing technique that involves a second phase in the densification of PZT, it was convenient to choose a PZT composition having a simple detectable X-ray pattern. The $PZ_{.5}T_{.5}$ composition was therefore selected because of its tetragonal perovskite lattice structure and its center position within the $PbZrO_3$-$PbTiO_3$ phase system. In addition, the $PZ_{.5}T_{.5}$ composition was also chosen because at the PbO deficient side of its single phase width, a nonstoichiometric material exists consisting of both rhombohedral and tetragonal phases.[31] As a result, X-ray analysis can be used to detect when the $PZ_{.5}T_{.5}$ composition reaches equilibrium with the PbO deficient side of its single phase width.

The lead oxyfluoride composition, $PbO{\cdot}PbF_2$, was considered for the rearrangement and liquid phase sintering steps in densifying PZT because of the following characteristics:

(1) The composition has a low melting temperature of approximately 500°C. The low melting temperature allows the use of a relative economical hot-press die (stainless steel) to provide the pressure needed to enhance the rearrangement process on melting of the second phase material.

(2) The composition on melting contains PbO that would provide for the solubility of solid PZT needed for rapid liquid phase densification.

(3) The vapor pressure of PbF_2 is greater than that of PbO. At high temperatures the PbF_2 can readily evaporate from the system leaving a rich PbO liquid whose evaporation could be influenced by an external PbO atmosphere.

(4) The $PbO \cdot PbF_2$ composition has been used successfully as a flux for growing single crystals in the PZT system.[39,40]

A. Powder Characterization

In the preparation of the mixed oxides $PZ_{.5}T_{.5}$, a high calcining temperature of 1200°C was chosen to insure complete reaction of the oxides. This provided a means of definitely distinguishing the X-ray peaks of $PZ_{.5}T_{.5}$ from that of the liquid phase after the initial hot-pressing step in the densification process. Also, due to the high calcination temperature, a large particle size $PZ_{.5}T_{.5}$ material was developed that provided a comparison on densifying submicron particles $PZ_{.5}T_{.5}$ made from chemically prepared material. Table II gives the specific surface area of the materials after powder preparation.

The lead oxyfluoride composition was prepared from PbO and PbF_2 powder mixed in distilled water by the reaction:

$$PbO + PbF_2 + 3H_2O \xrightarrow[25°C,\ 24\ hrs.]{\text{hydrolysis}} 2\ Pb(OH)_2 + 2HF \xrightarrow[110°C,\ 24\ hrs.]{\text{dry}} Pb_2OF_2 + 3H_2O\uparrow$$

This procedure provided a uniform "liquid" phase composition by preventing a heat treatment that might have caused PbF_2 evaporation.

In preparing the chemically prepared $PZ_{.5}T_{.5}$, it was necessary to determine the correct amount of ZrO_2 and TiO_2 in solutions of $Zr(OBu)_4$ and $Ti(OBu)_4$, respectively, to obtain the desired Zr/Ti ratio during mixing. This was accomplished by forming a precipitate from a known volume of the metal tetrabutoxide by adding distilled water. A heat treatment to remove the chemical water and carbonaceous impurities from the precipitate, and thereby form the oxide, gave 28.4 w/o ZrO_2 and

TABLE II

Material	Specific Surface Area (m^2/g)	Green* Density at 10,000 psi (% of theoretical)
Mixed Oxides $PZ_{.5}T_{.5}$	0.12	59.8
Chemically Prepared $PZ_{.5}T_{.5}$	8.3	30.6
$PbO \cdot PbF_2$	1.1	

*Average geometric density of all $PZ_{.5}T_{.5}$ + X wt% $PbO \cdot PbF_2$ after cold pressing.

23.4 w/o TiO_2 for the respective metal tetrabutoxide.

After mixing the correct proportions of $Zr(OBu)_3$, $Ti(OBu)_4$, and PbO to form $PZ_{.5}T_{.5}$ along with isopropyl alcohol, water was added slowly to precipitate a white powder which was characterized by TG, DTA, and X-ray diffraction after calcining at various temperatures. Figure 4a shows the weight loss observed with temperature for the chemically prepared powder. A total weight loss of 5% occurred within the temperature range of 50° to approximately 500°C and was attributed to the loss of surface-absorbed water and the removal of carbonaceous material. Comparing the weight loss curve with the DTA data of Fib. 4b, it was observed that an endothermic peak exists between 100° and 200°C indicating dehydration of the powder. At approximately 325°C a strong exothermic peak occurs and compares in temperature to the remaining weight loss range shown thermogravimetrically. Removal of the last of the chemical water and carbonaceous impurities allows the exothermic reaction associated with crystallization of the material to occur.

X-ray examination of the powder after various heat treatments showed the crystallization character of the chemically prepared $PZ_{.5}T_{.5}$. A heat treatment at 250°C gave an X-ray pattern of an amorphous powder having a very broad single peak. By heating the precipitate powder to 350°C, broad X-ray peaks appeared that related to the beginning of PZT crystallization as indicated by the large exothermic peak of Fig. 4b. A further heat treatment at 450°C showed a narrowing of the broad peaks corresponding to unreacted PbO and ZrO_2. It is suggested that since the initial solution in the preparation of the chemically prepared $PZ_{.5}T_{.5}$ contained a PbO powder instead of a lead alkoxide, the lead was not

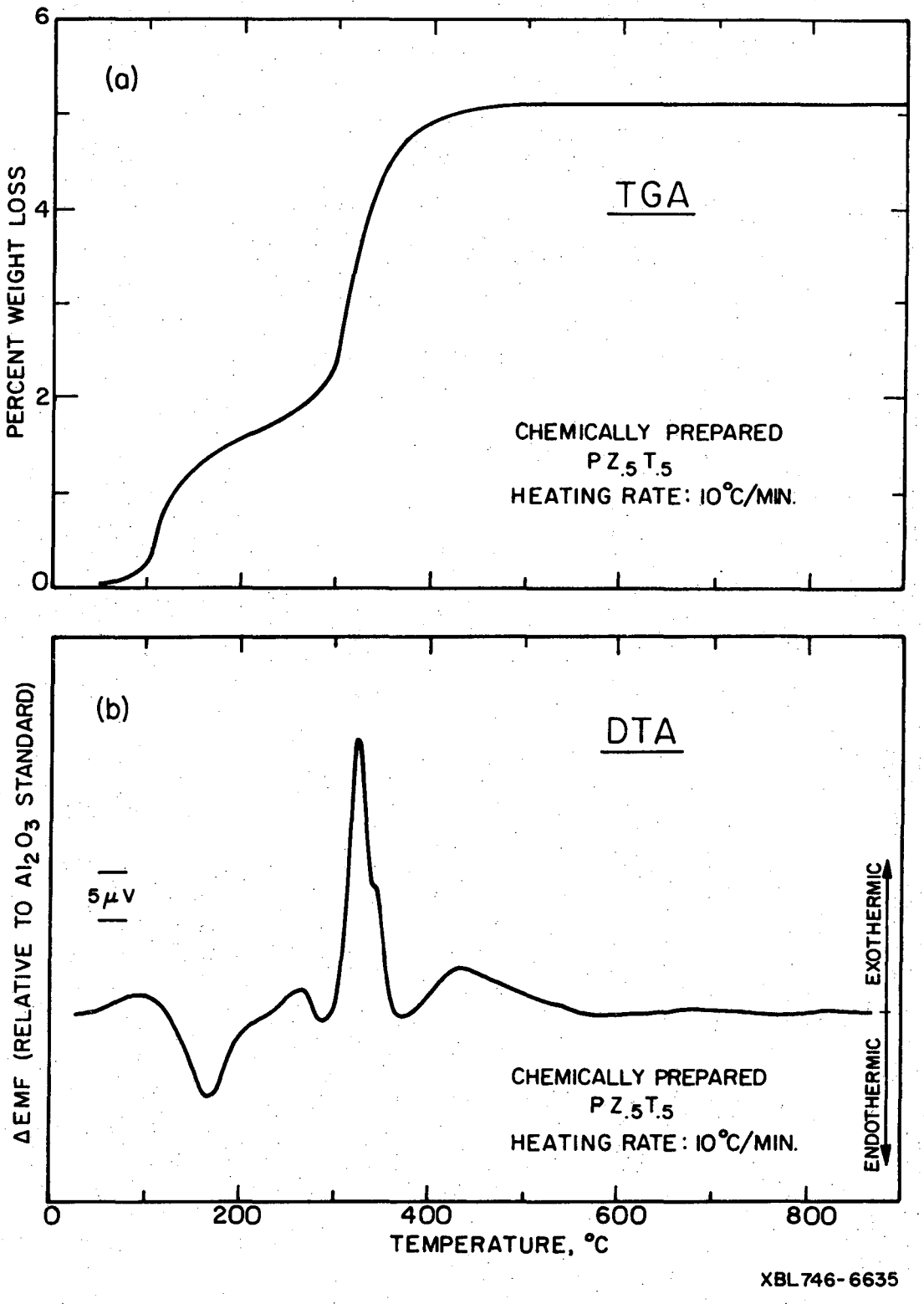

Figure 4. Powder characterization representing both (a) weight loss behavior and (b) differential thermal behavior of the chemically prepared powder.

intimately mixed to provide complete reaction. Hence, some of the PbO must rely on an extended diffusion process to form the PZT composition. This interpretation is supported by the broad exothermic peak of Fig. 4b from 375° to 550°C.

B. Liquid Phase Pressing

The first step in the liquid phase densification technique is essentially concerned with the removal of porosity in the initial PZT compact by optimizing, with the aid of applied pressure, the rearrangement process associated with formation of a liquid phase. The objective of this procedure was to prepare the PZT sample for rapid liquid phase sintering by establishing a high initial density. This was accomplished by pressing the PZT sample containing $PbO \cdot PbF_2$ within zirconia sand at 600°C using a stainless steel hot press die assembly as shown in Fig. 2. The zirconia sand prevented stresses from occurring in the sample on cooling due to the mismatch in thermal expansion with stainless steel. The sand also provided easy removal of the sample from the die after hot pressing.

Cook and Dungan[41] have used a similar die geometry in hot pressing PZT embedded in zirconia sand using an alumina die. By the use of strain gages, they showed that only about 50% (depending on sand mesh) of the applied load was actually transmitted to the sample in the vertical direction. The force along the horizontal direction remained very low. As a consequence, displacement of the sample was largely in the direction of the applied load with very little change in the initial diameter. In pressing $PZ_{.5}T_{.5}$ in the presence of a liquid phase using a stainless steel insert, the displacement of the pressed sample was also found to

be mainly in the direction of the applied load.

A typical comparison of displacement of the $PZ_{.5}T_{.5}$ sample versus time at 600°C for the mixed oxides and chemically prepared materials, with and without the liquid phase, is shown in Fig. 5. It is observed that in both $PZ_{.5}T_{.5}$ powder preparations the presence of a liquid phase greatly increases the densification of the sample. The data also show that the fine particle chemically prepared powder has a much higher displacement as compared to the mixed oxide material. This is probably a result of the very low green density obtained in the chemically prepared material as presented in Table II which is characteristic of submicron particle size materials.[42]

The data of Fig. 5 also show a pressing run performed in air for the mixed oxides sample. Original experiments in the investigation of liquid phase pressing at 600°C were attempted in both O_2 and in air. By slicing through these pressed samples, it was observed that the center region had a black appearance. From X-ray examination, it was found that the black region contained some metallic lead that existed even in samples pressed in an oxygen atmosphere. Since any substitution of F^{-1} for O^{-2} into the PZT structure must result in excess PbO:

$$Pb(Zr_{.5}Ti_{.5})O_3 + x\ PbF_2 \rightarrow Pb_{1-x}\ \square_x\ (Zr_{.5}Ti_{.5})O_{3-2x}\ F_{2x} + 2xPbO$$

where $\square$ represents the vacancy for charge compensation, it was assumed that the presence of metallic lead was due to the high percentage of PbF_4 that exists in the vapor phase of PbF_2. Zmbov et al.[43] and Hauge et al.[44] have shown that the vapor phase of PbF_2 at 715°C contains 66%

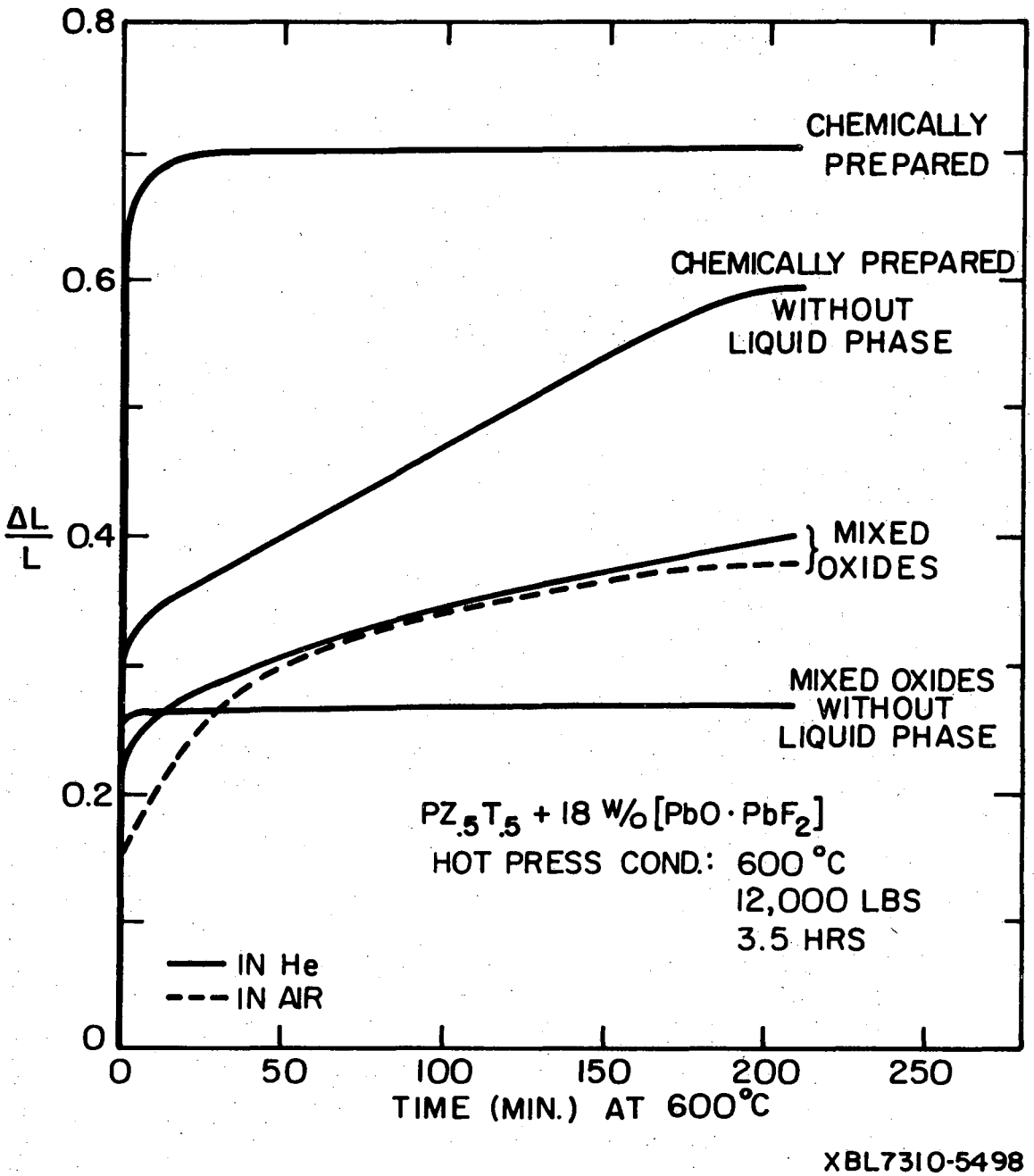

Figure 5. Comparison of displacement versus time for both the mixed oxides and chemically prepared materials.

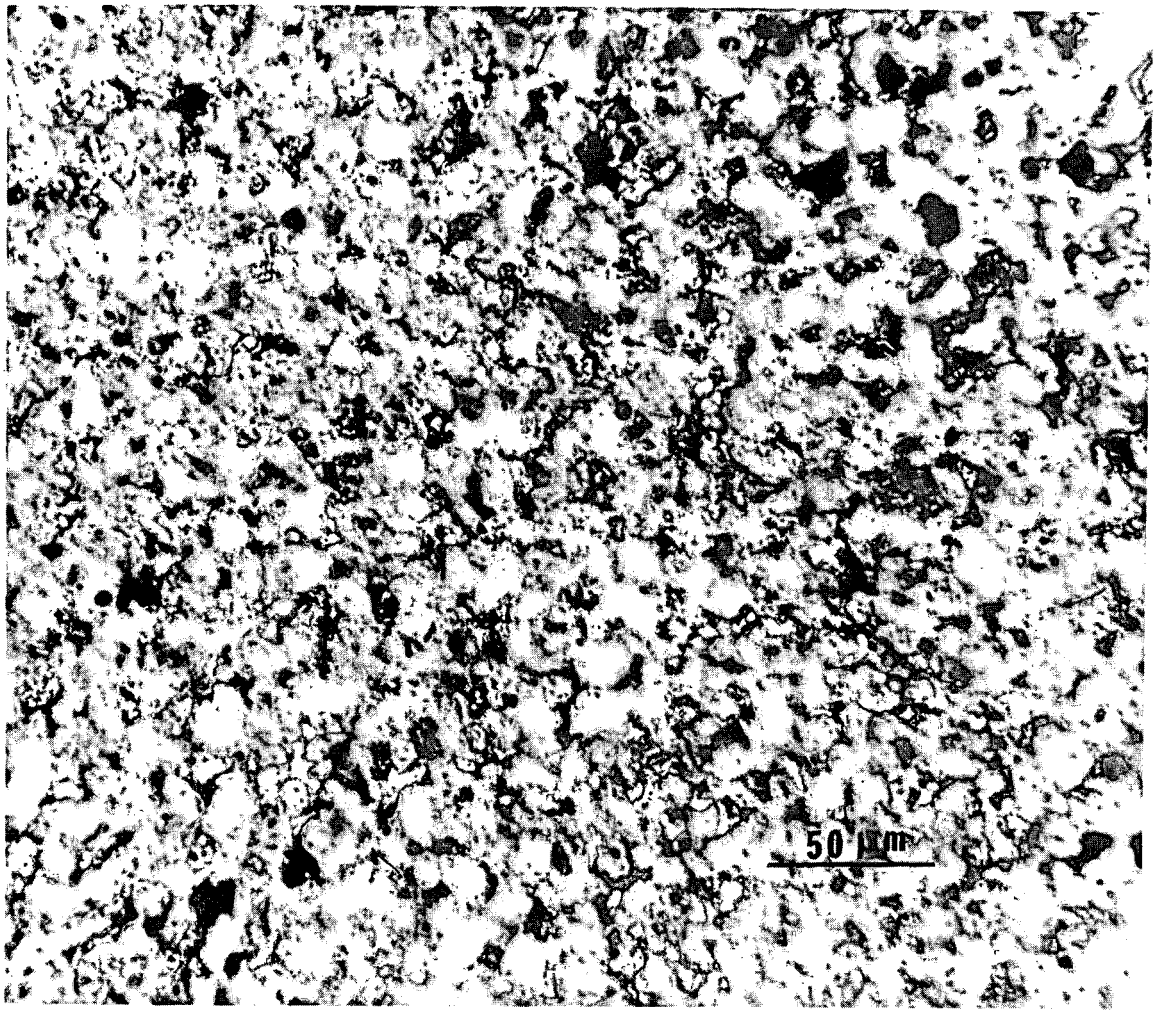

XBB 746-4290

Figure 6. Photomicrograph of $PZ_{.5}T_{.5}$ prepared from mixed oxides after hot pressing at 600°C.

PbF_4, 25% PbF_2, 2% PbF, and 7% Pb. Evaporation of PbF_2 from liquid $PbO{\cdot}PbF_2$ can therefore develop a partial pressure of lead in the system. During hot pressing, the sample densifies to the extent that oxidation of this lead must proceed by diffusion through the compact. As a result, the appearance of the black region of the center of the sample after pressing indicates where oxidation of the lead has not occurred. In any case, pressing in helium gave a uniform blackness throughout the samples and also a slightly greater displacement. Hence, all hot pressings were performed in helium. A photomicrograph of the mixed oxide prepared $PZ_{.5}T_{.5}$ sample after pressing is presented in Fig. 6 showing very light areas that are probably metallic lead. The black areas are "pull-outs" of material due to polishing.

To determine the optimum liquid content for the first step in the process, samples of both powder preparations were hot pressed with various weight percents of $PbO{\cdot}PbF_2$. The optimum initial amount of liquid phase was established by comparing the density of the pressed $PZ_{.5}T_{.5}$ after removal of the liquid by TG.

C. TG Liquid Phase Removal

The method of determining the amount of liquid remaining in the pressed samples was based on the weight loss behavior of a two-phase system where the activity of a volatile component at a constant temperature must remain constant. The $PbO\text{-}ZrO_2\text{-}TiO_2$ isothermal ternary phase diagram at 1100°C[16,45,46] is shown in Fig. 7, along with the single phase width for $PbZr_xTi_{1-x}O_3$.[30] At 1100°C an initial PZT sample with excess PbO will lie in the two-phase region represented by solid PZT and a PbO rich liquid. Because PbO has a significant vapor pressure at 1000°C,

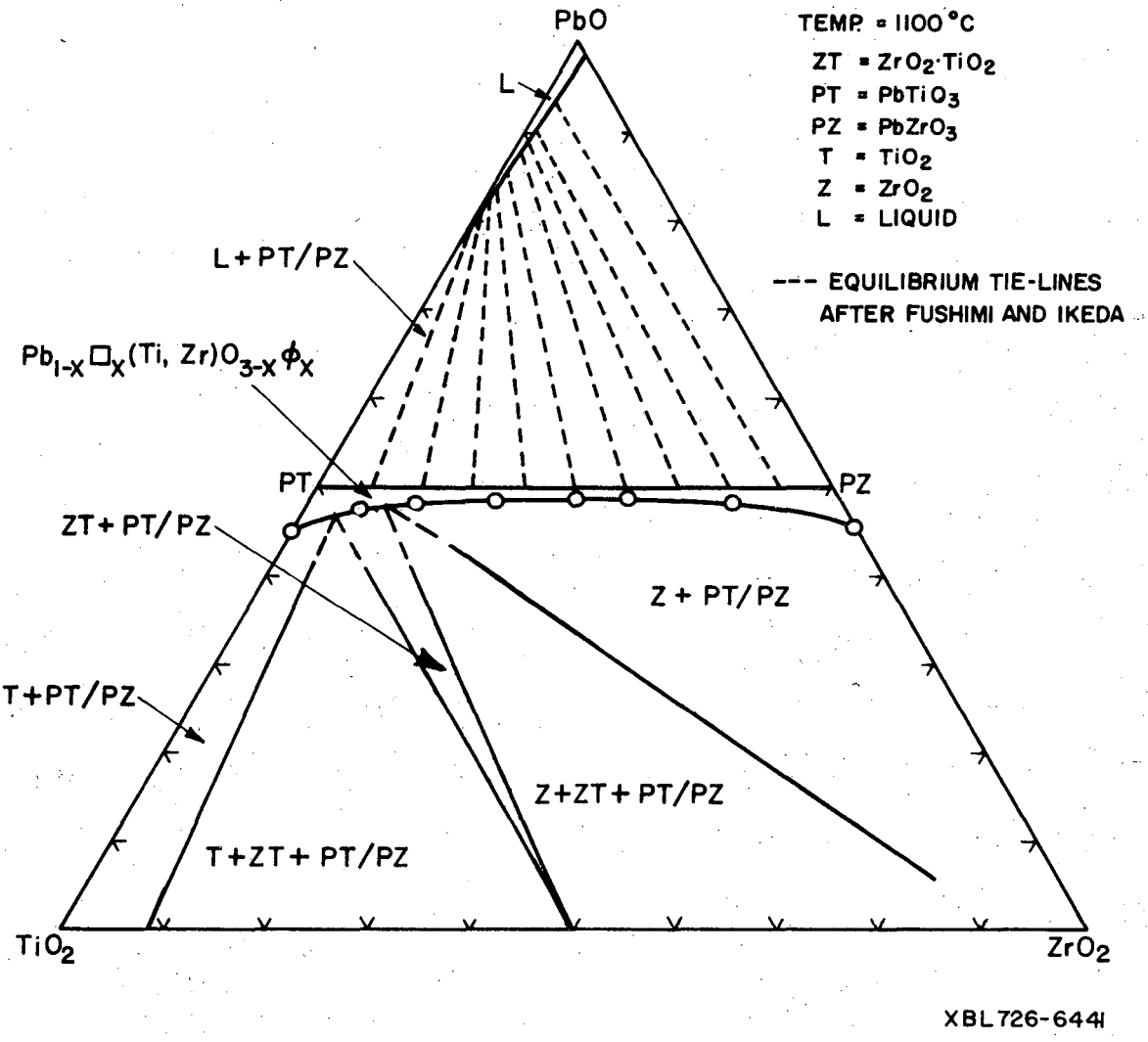

Figure 7. Isothermal ternary phase diagram of PbO-ZrO_2-TiO_2 at 1100°C (the diagram is reproduced from Holman and Fulrath[30]).

the loss of PbO by evaporation from the system will eventually reduce the amount of liquid and leave only the solid PZT. During the time that the two phases exist in equilibrium, the vapor pressure or activity of PbO, a_{PbO},* must remain constant. This point can be more clearly emphasized if it is assumed that a "quasi-binary" analysis of a designated PZT composition is applicable to the type of binary phase diagram represented by PbO-TiO_2 shown in Fig. 8a.

A constant temperature line across the phase diagram at 1100°C shows points A, B, C, and D at different isothermal compositional positions. At point A, a two-phase region consisting of a PbO rich liquid and solid PT are in equilibrium. Upon loss of PbO by evaporation, point A approaches point B indicating that the amount of liquid phase has been reduced (lever rule) but that the solid phase compositions are unchanged as defined by the equilibrium phase diagram. Since the composition of the liquid and solid phases remain unaltered (only their relative amounts change) the activity of PbO remains constant as shown in Fig. 8b.** Further loss of PbO will remove the liquid entirely leaving only a single phase PT solid of width ΔW represented by points B and C. In this region, loss of PbO introduced nonstoichiometry within the PT solid by generating both lead and oxygen vacancies:

$$Pb_{1-x} \square_x Ti\ O_{3-x} \phi_x$$

---

* The activity of PbO above the PZT system is defined:

$$a_{PbO}(PZT) = P_{PbO}(PZT)/P_{PbO(pure)}$$

** At constant temperature, the activity is only a function of composition.

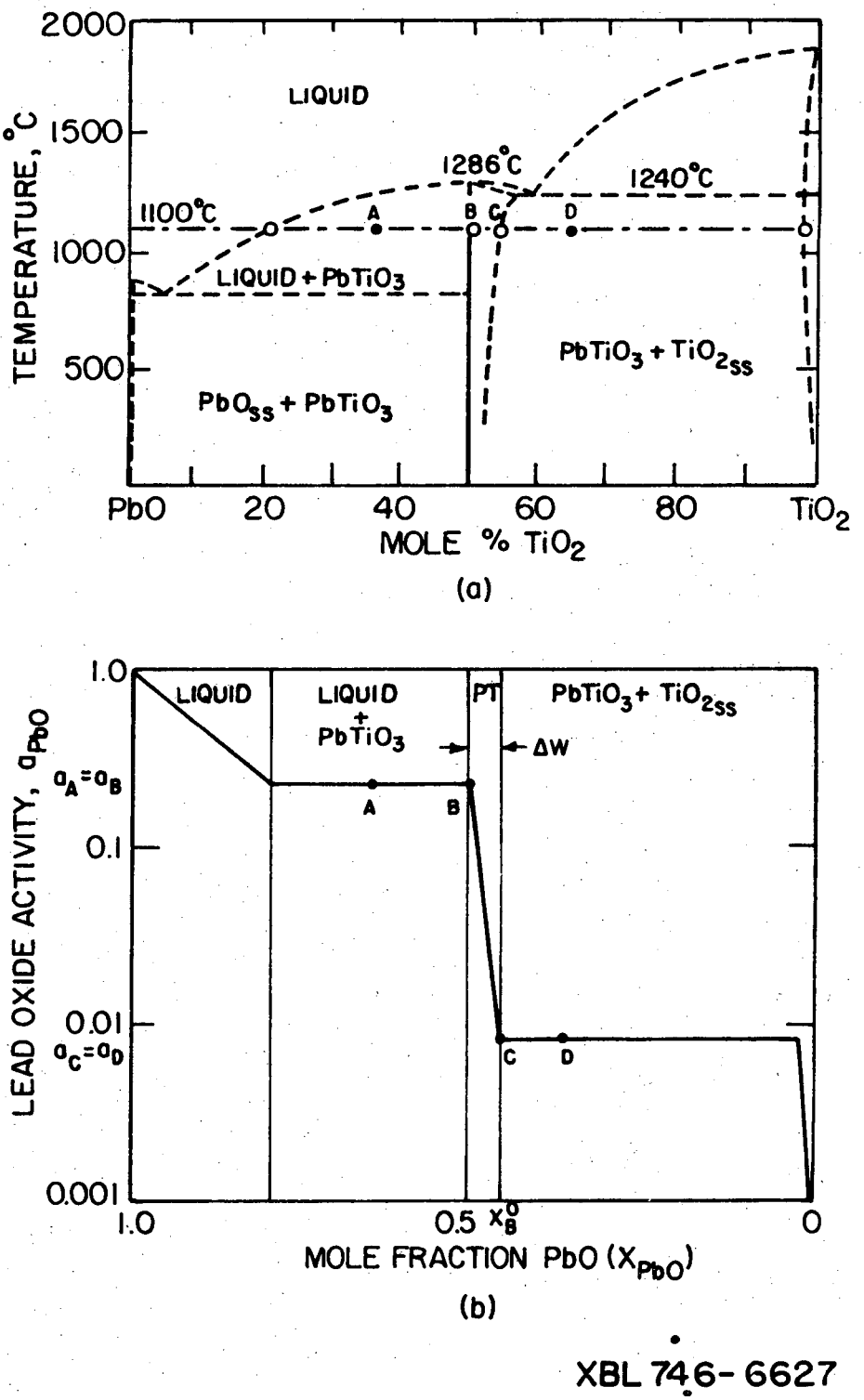

Figure 8. (a) Proposed $PbO-TiO_2$ phase diagram after Moon[18] and Holman and Fulrath.[30]
(b) Activity of PbO versus mole fraction of PbO at 1100°C for the $PbO-TiO_2$ binary.[30]

where $\square$ and ϕ represent lead and oxygen vacancies respectively. The resultant change in composition in this region lowers the PbO activity until point C is reached. At point C the loss of PbO is sufficient to begin nucleation of a second phase of solid TiO_2 if further evaporation occurs. Between points C and D within the region of two solid phases, the compositions again remain constant, fixing the PbO activity. Since the activity of PbO defines the vapor pressure of PbO above the system (based on the standard state of pure PbO), a constant activity refers to a constant vapor pressure, and thus, a varying activity implies a pressure change. Consequently, a multiple phase region in the PZT system asserts a constant vapor pressure of PbO while a single phase region produces a variable PbO pressure.

Because the vapor pressure of a system is related to the rate of weight loss from the system, detection of both types of phase regions can be realized by means of thermogravimetry. The high vapor pressure species must have sufficient molecular weight to produce measurable weight changes as in the case of the PbO vapor. From the Langmuir equation which is based on the concept that when a system is in equilibrium the number of molecules leaving a surface is independent of the molecules striking the surface, the vapor pressure is proportional to the rate of weight loss at constant temperature.[47] Hence, for a constant vapor pressure (two-phase region) the rate of weight loss is linear and for a variable pressure (single phase region) the rate is non-linear.

The discussion thus far has been based on the weight loss behavior of PZT in the presence of a PbO rich liquid phase without considering the effect of PbF_2. With the addition of an initial $PbO{\cdot}PbF_2$ phase to PZT,

the weight loss behavior is similar to that of PZT plus PbO: The PZT sample after pressing contained on cooling solid additional phases of metallic lead, lead fluoride and lead oxyfluoride. On heating this sample in air, the metallic lead oxidizes to form PbO. At approximately 500°C, the lead oxyfluoride begins to melt, allowing some of the PbO along with the PbF_2 to dissolve in the liquid. When this happens, and since PbF_2 has a much higher vapor pressure than PbO, the composition of the liquid phase on further heating becomes increasingly rich in PbO. As a result, the comparison in weight loss behavior of the sample with that of a PbO rich liquid without PbF_2 is similar, especially when the PbF_2 can evaporate independent of the PZT system as experimental evidence will later indicate. An example of the weight loss behavior of a $PZ_{.5}T_{.5}$ sample containing the liquid phase after hot pressing is illustrated in Fig. 9. When the observed rate of weight loss of the sample is linear, the vapor pressure of PbO is constant and the sample is in the two-phase region (ignoring the PbF_2). The linear weight loss rate continues until the composition of the sample enters the single phase region where the vapor pressure is not constant and a non-linear rate of weight loss occurs. Development of a second phase due to further loss of PbO establishes once again a linear weight loss rate. By extending the slope of the linear rates, the points of tangency to the curve bracket the constand temperature single phase width, ΔW, for the $PZ_{.5}T_{.5}$ sample.[30]

In comparing the amount of liquid phase content after hot pressing in samples of various initial weight percent of $PbO \cdot PbF_2$, the percent amount was determined based on the same instantaneous vapor pressure of PbO within the single phase width. This was achieved by establishing

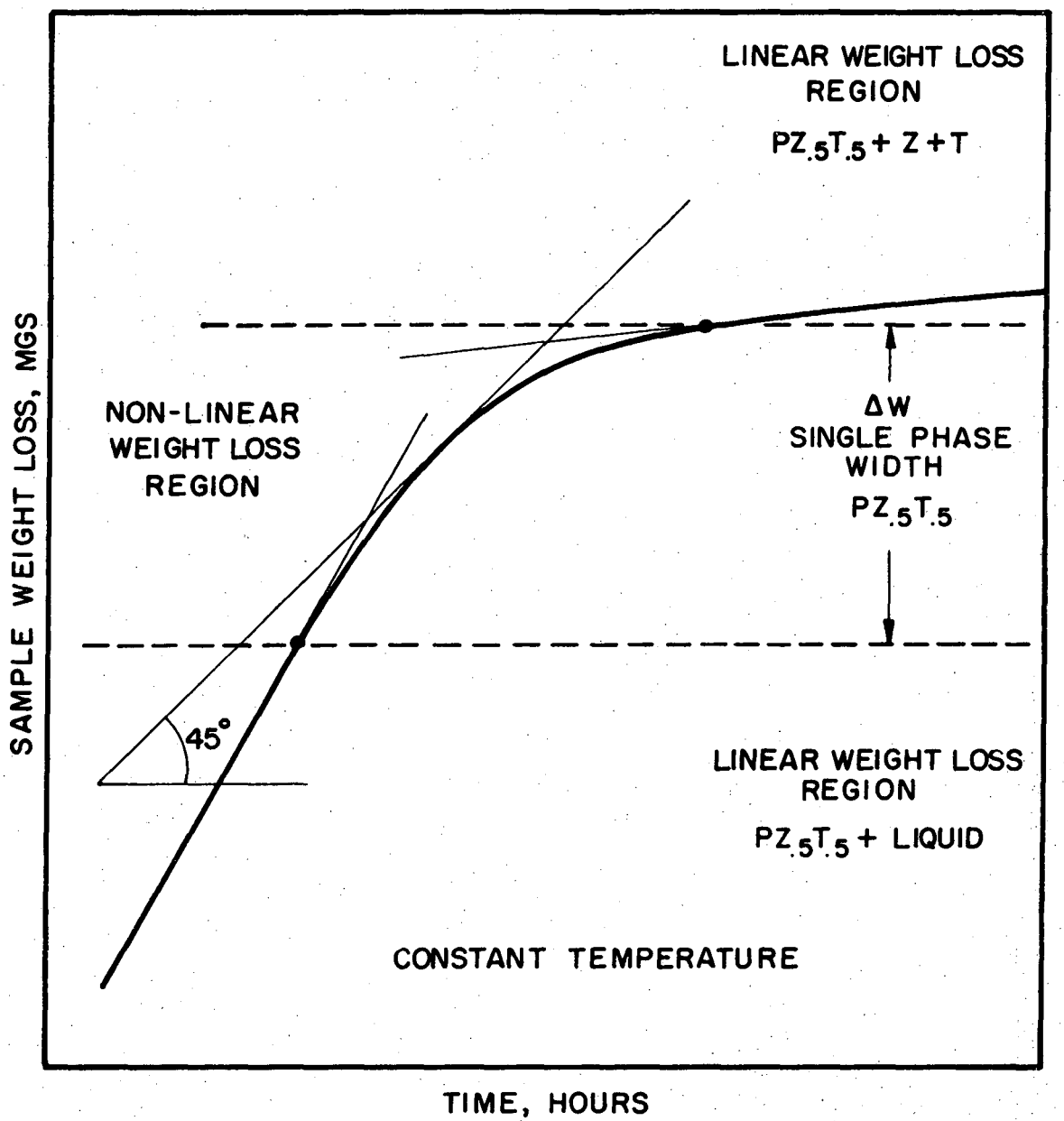

Figure 9. Typical weight loss behavior after hot pressing of a $PZ_{.5}T_{.5}$ specimen containing the liquid phase.

the point within the single phase width that permitted a tangent with a 45° angle as illustrated in Fig. 9. Although the true liquid amount is less than that determined by this method, the relative comparison between samples was found to be more convenient and more accurate by this procedure.

Using the liquid removal method by thermogravimetry, the weight percent liquid phase remaining after pressing versus the initial weight percent of $PbO{\cdot}PbF_2$ before pressing is given in Fig. 10a for both the mixed oxides and chemically prepared $PZ_{.5}T_{.5}$. The lower percent liquid loss of the chemically prepared powder was a result of its high displacement, as typified in Fig. 5, from a starting low green density that allowed some of the liquid to be pressed out of the sample. From a measurement of the density of the specimens after removal of the liquid phase, the optimum amount of initial $PbO{\cdot}PbF_2$ content was established from the data represented by Fig. 10b. For the chemically prepared $PZ_{.5}T_{.5}$, it was observed that a relative density as high as 98% was obtained for an initial 18 wt% $PbO{\cdot}PbF_2$ addition; an initial 22 wt% liquid phase gives a relative density of 82% for $PZ_{.5}T_{.5}$ made from mixed oxides. These highest green densities were chosen as the optimum liquid content for low temperature liquid phase pressure sintering. The decrease in the density for high liquid additions greater than the optimum was thought to be due to the continuous increase in the volume fraction of liquid which, on removal, increases the amount of porosity.

D. Controlled Liquid Phase Sintering

With the proper amount of second phase addition established, the ability of removing the liquid phase in a controlled manner while liquid

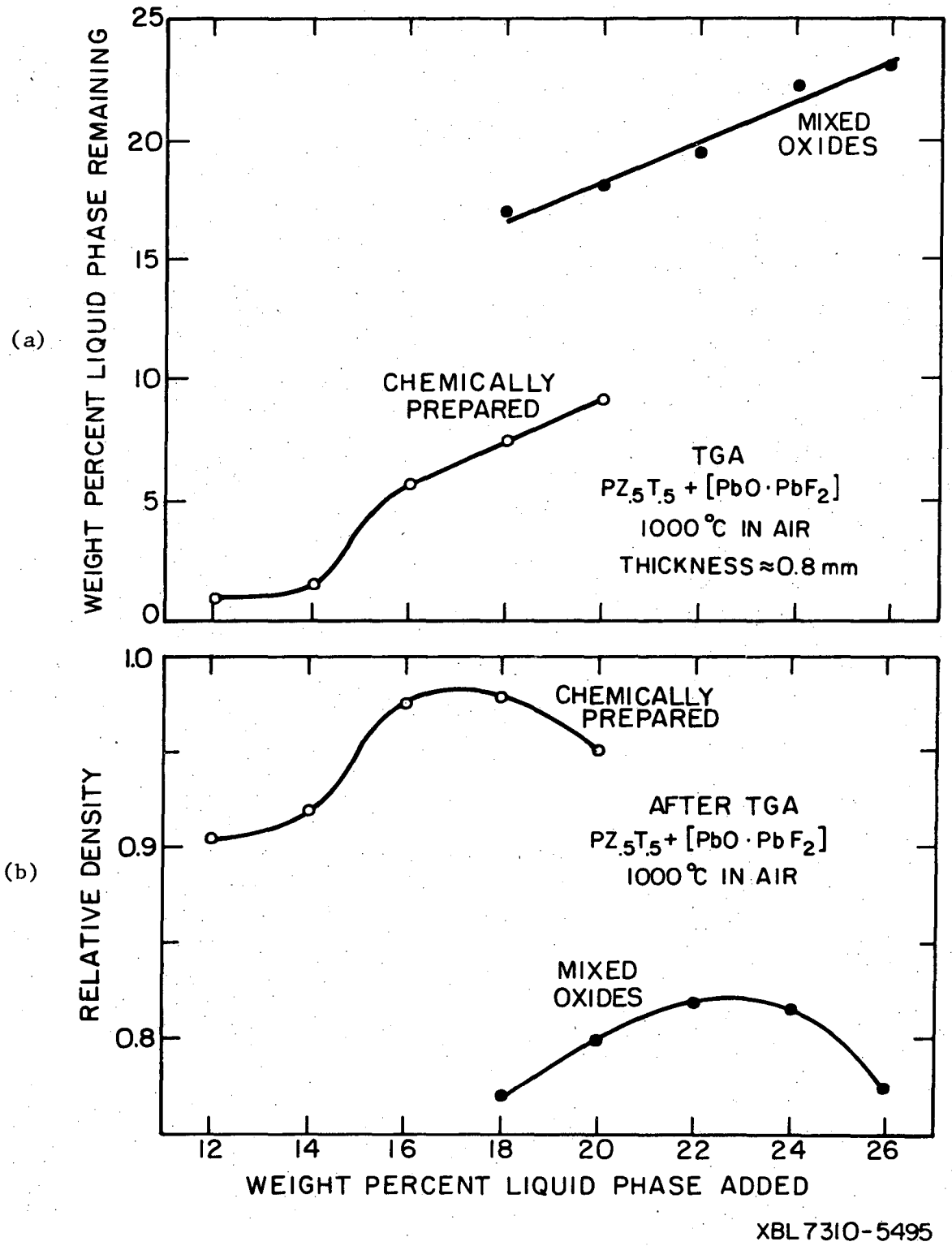

Figure 10. (a) Amount of liquid phase remaining in samples after hot pressing as determined by thermogravimetry.
(b) Comparison of resultant densities after liquid removal.

phase sintering was investigated by a subsequent heat treatment within a fixed PbO atmosphere. A constant PbO atmosphere was maintained at constant temperature by using various multi-phase packing powder compositions within the PZT system. The compositions were chosen to create atmospheres of various PbO activities that would allow a sample to attempt to equilibrate by losing PbO, yet maintain the sample in its single phase region.

The choices of multi-phase packing powder compositions were determined for use with $PZ_{.5}T_{.5}$ from experimental Knudsen effusion vapor pressure data shown in Fig. 11.[30] The data shows the lead oxide activity as a function of reciprocal temperature for initial multi-phase compositions within the PZT system. It is of interest to note that on the high PbO composition side of the ternary where a rich PbO liquid phase can form, the lead oxide activity decreases with an increase in temperature. This is a result of the change in liquid composition due to an increase in the solubility of titania and zirconia with increasing temperature which lowers the relative amount of PbO in the liquid phase.

(1) Single Phase Activity Width

The data of Fig. 11 give the lead oxide activity of $PZ_{.5}T_{.5}$ for both a high and low PbO composition region with increasing temperature. Because the activity of PbO is constant within a multi-phase region, the PbO activity line for the starting $PZ_{.5}T_{.5}$ + PbO composition sets the high PbO activity side of the single phase width of $PZ_{.5}T_{.5}$ with temperature. Similarly, the PbO activity line for the $PZ_{.5}T_{.5}$ + Z + T composition indicates the low PbO activity side of the single phase width of $PZ_{.5}T_{.5}$ at different temperatures. Consequently, for a constant

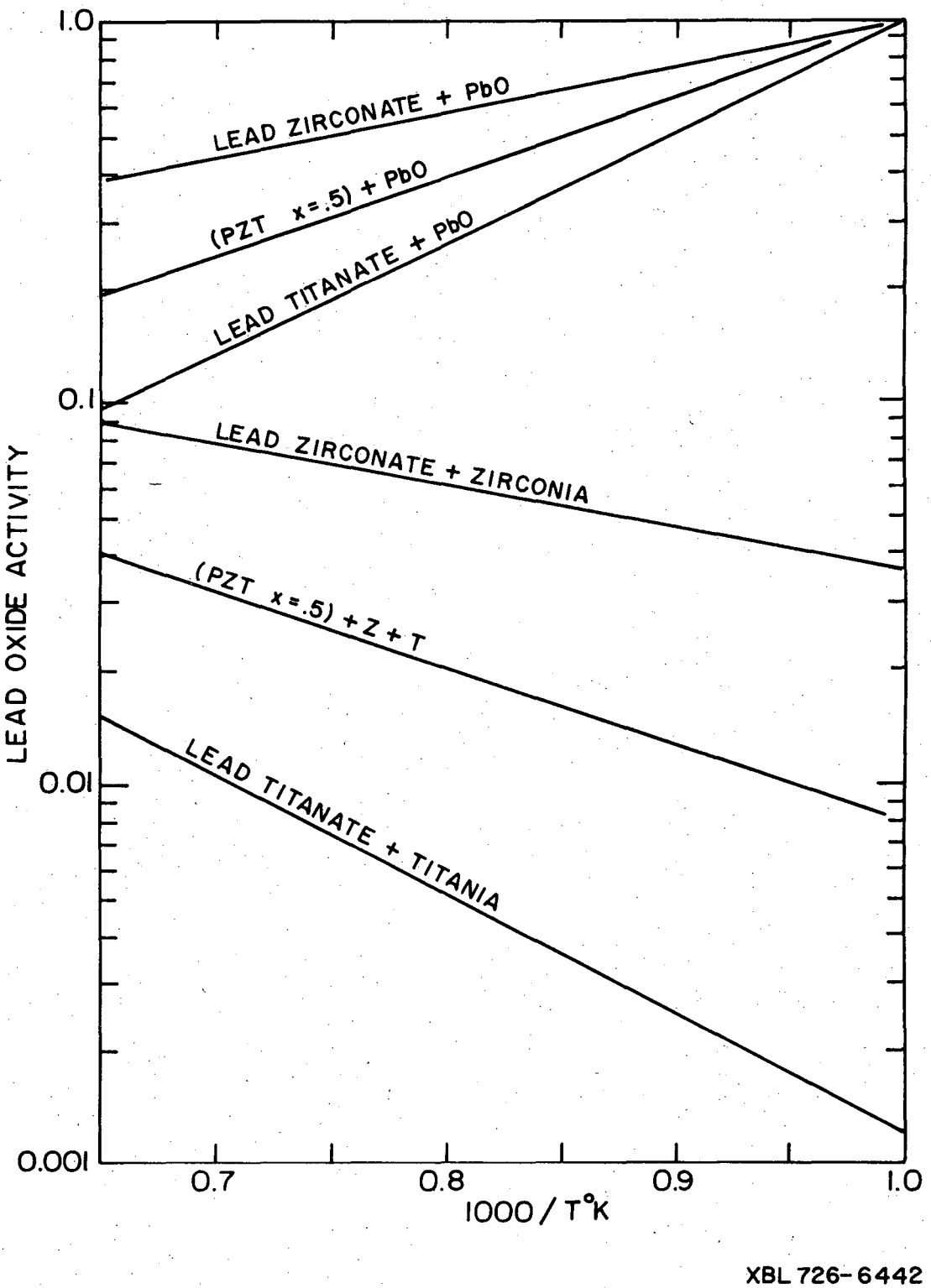

Figure 11. Lead oxide activity versus reciprocal temperature for the PZT system (reproduced from Holman and Fulrath[30]).

temperature, the activity difference between the two multi-phase $PZ_{.5}T_{.5}$ compositions represents the PbO activity width of the single phase region of $PZ_{.5}T_{.5}$.

During liquid phase sintering, the PbO activity of a $PZ_{.5}T_{.5}$ sample containing the liquid phase is essentially on the high PbO activity side of its single phase region. If the sample is isothermally sintered within a packing powder environment having an activity of PbO less than that of the sample, the sample will proceed to equilibrate by losing PbO until its PbO activity matches that of the packing powder. By selecting a packing powder composition that has a lower activity of PbO than the sample but greater than the low PbO activity side of the single phase region of $PZ_{.5}T_{.5}$, loss of PbO will set the $PZ_{.5}T_{.5}$ sample composition within its single phase region as determined by the PbO activity of the packing powder.

From Fig. 11 it is observed that both the PZ + Z and the PT + P packing powder compositions have PbO activities that exist within the activity difference of the single phase width of $PZ_{.5}T_{.5}$. Other multi-phase compositions also exist within this single phase activity region, e.g., compositions of $PZ_x T_{1-x}$ + P and PZ_{1-x} + Z + T_y where $o \leq x \leq .5$ and y = o only when x = o. Thus there is a PbO activity region within the single phase width of $PZ_{.5}T_{.5}$ that appears as an activity gap between the PZ + Z and the PT + P compositions. It is evident that for any PZT material the intrinsic nonstoichiometric composition cannot be fixed in this region of the single phase width by a packing powder composition in the PZT system. This may be overcome by performing Knudsen effusion experiments to determine the PbO activities of multi-phase PZT

compositions containing dopants. It is expected that dopants creating lead site vacancies will lower the PbO activity of a PZT + P packing powder composition and possibly remove this existing activity gap.

(2) Effect of Activity Difference

The effect of removing the liquid from a mixed oxide prepared $PZ_{.5}T_{.5}$ sample during liquid phase sintering was considered for packing powder compositions in the $PZ_{.5}T_{.5}$ single phase PbO activity width. The compositions chosen were PZ + Z, PT + P, and a "control experiment" packing powder of $PZ_{.5}T_{.5}$ + P having the same PbO activity as the sample. Use of the $PZ_{.5}T_{.5}$ + P packing powder composition provided information on the ability of the experiment to correctly control the activity of the PbO atmosphere and, thereby, influence the weight loss behavior of the sample.

The results of the study are presented in Fig. 12a where the fraction of liquid removed versus time at 1200°C is shown for a slow heating rate of 86°C/hr. For the PZ + Z packing powder composition where the PbO activity difference from the sample is large, all the liquid was removed before reaching temperature. This result is reflected in the data of Fig. 12b where the relative density of the sample has not changed from that obtained from the first step of the process, suggesting very little liquid phase sintering has occurred. Thus, the large PbO activity difference between PZ + Z and the sample does not allow sufficient retention of the liquid phase to provide enhanced densification. The PZ + Z packing powder acts as a large PbO sink forcing the sample to give up its liquid phase, whereby densification can only proceed by a solid state mechanism.

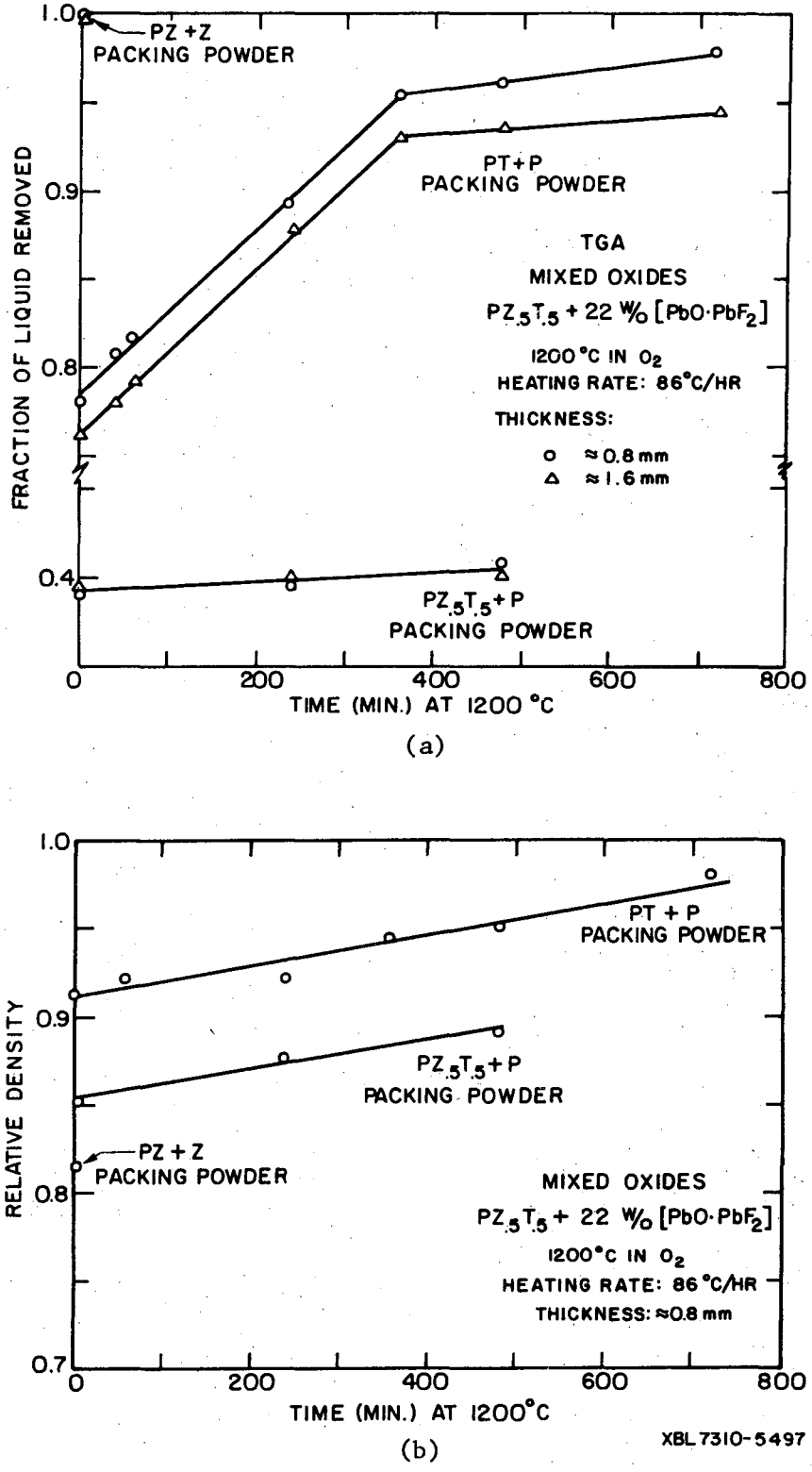

Figure 12. (a) Rate of removal of the liquid phase from $PZ_{.5}T_{.5}$ due to various multi-phase packing powder compositions.
(b) Comparison of density after removal of the liquid.

To study the liquid removal behavior in the presence of packing powders containing excess PbO, it was necessary to insure that the PbO activities of the powders remain constant at temperature. It was therefore necessary to determine how long during the heat treatment that the packing powder composition would remain two-phase. This was found by measuring the leak rate of the PbO vapor from the covered platinum crucible at temperature. The leak rate was measured by TG on the actual crucible used during the experiment. The highest PbO activity composition used in the experiment, $PZ_{.5}T_{.5}$ + P, showed a leak rate from the crucible of 18.6 mg/hr. indicating that the composition would remain two-phase for approximately 54 hours at 1200°C for 20 grams of an initial 5 wt% excess PbO addition.

In the case of the PT + P packing powder composition, the difference in PbO activity from that of the sample is less. Hence, it was observed, as shown in Fig. 12a, that the difference in PbO activity was small enough to influence the rate of liquid removal from the $PZ_{.5}T_{.5}$ sample. The rate of liquid removal appears to be linear although the rate changes after six hours. The relative density, after total liquid removal by TG, tends to continuously increase. A density as high as 98% was achieved with 12 hours for the mixed oxide prepared $PZ_{.5}T_{.5}$ material.

The "control experiment" packing powder composition, $PZ_{.5}T_{.5}$ + P, was an informative experiment on the ability to control the PbO portion of the liquid in the sample. The PbO activity of both the sample and packing powder are the same; thus, loss of PbO from the sample should be negligible as long as the packing powder remains two-phase and provides for a constant activity of PbO. From the data of Fig. 12a, the

predicted behavior was essentially observed where the fraction of liquid removed from the sample was relatively constant. Yet it is noted that approximately 40% of the liquid was removed from the sample. Since only the PbO vapor pressure of the sample can be influenced by the packing powder, PbF_2 will readily evaporate from the system. This indicates that after pressing at 600°C for 3.5 hours the liquid composition (after a subsequent oxidation of the metallic lead) contained 60% PbO and 40% PbF_2 instead of the original 50-50 composition.

(3) Effect of Thickness

The data of Fig. 12a showing the fraction of liquid removed with time was obtained from mixed oxide $PZ_{.5}T_{.5}$ specimens having a thickness of approximately 0.8 mm and 1.6 mm. For the PZ + Z packing powder composition, the complete loss of liquid from the specimens before reaching temperature was the result found for both thicknesses. The activity difference between PZ + Z and the specimen, therefore, allowed total removal of the liquid independent of thickness within the range investigated. In the case of the PT + P composition where the activity difference from the specimen was small, the rate of PbO loss was initially thickness independent. Yet upon reaching a relative specimen density of approximately 94%, where a closed pore condition develops, the rate of PbO loss becomes thickness dependent. The separation in the fraction of liquid removed between the specimens of different thickness was due to the larger amount of liquid in the thicker sample since the rate of PbO loss was constant. The $PZ_{.5}T_{.5}$ + P packing powder produces a negligible loss rate of PbO because of the same PbO activity as that of the sample. Hence, the fraction of liquid removed from the specimens remained the

same regardless of thickness.

The behavior in the rate of PbO loss due to sample thickness can be analyzed by considering a stepwise evaporation process that leads to a sample weight change:

$$PbO(b) \rightleftarrows PbO(s) \qquad (1)$$

$$PbO(s) \rightarrow PbO(g) \qquad (2)$$

where PbO(b) represents the PbO molecule within the bulk of the sample, PbO(s) represents the PbO molecule at the surface of the sample, and PbO(g) as the PbO molecule in the vapor.

When two different thickness $PZ_{.5}T_{.5}$ samples containing the liquid phase are heated in air during a TG experiment, the rate of weight loss appears as shown in Fig. 13. The rate of weight loss is thickness dependent and demonstrates that reaction (1) is rate limiting or the slowest reaction rate. By heating the sample in air, reaction (2) becomes the fastest process and hence the evaporation process must depend on the rate of reaction (1). If similar specimens are heated in an atmosphere of PbO created by a packing powder, i.e. PT + P, the rate of weight loss, as was indicated in Fig. 12a, becomes thickness independent. In this case, the activity of PbO developed by the packing powder decreases the rate of reaction (2) allowing the rate of reaction (2) to become rate controlling. Thus the evaporation process must depend on the rate of PbO leaving the surface of the sample which is a thickness independent process.

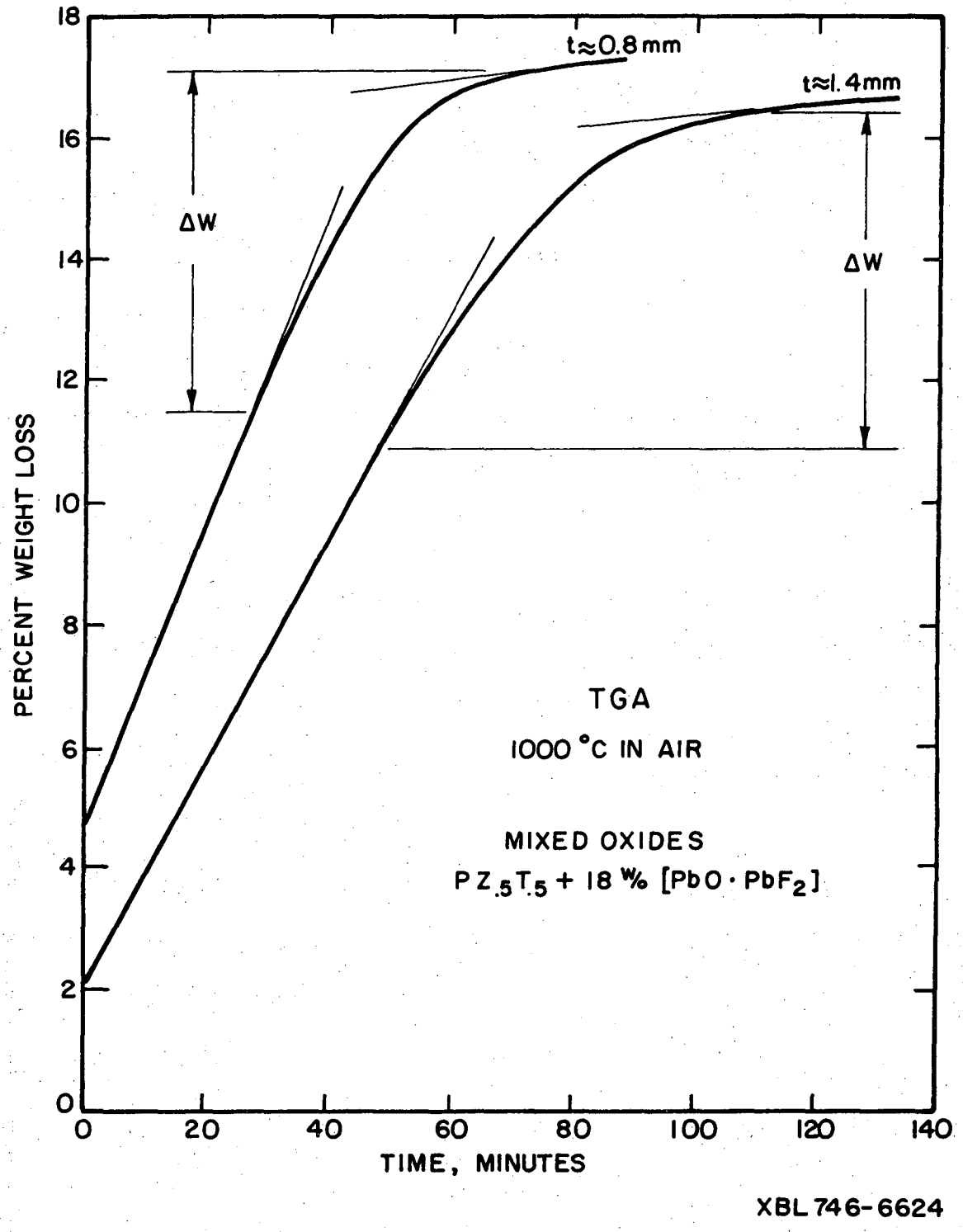

Figure 13. Rate of weight loss as a function of thickness of the $PZ_{.5}T_{.5}$ sample.

(4) Temperature Dependence

Specimens of mixed oxides prepared $PZ_{.5}T_{.5}$ were liquid phase sintered at various temperatures to determine the effect of temperature on the rate of liquid removal with time. Figure 14a gives the fraction of liquid removed versus time for different temperatures as determined by the TG method for establishing the amount of liquid remaining in the sample after sintering. For the specimens sintered at 1250°C, it was observed that after two hours a change in the rate of PbO loss was again present. This can again be contributed to the development of a closed pore geometry as indicated by the relative density of Fig. 14b. The relative densities for the specimens tend to continuously increase with time for the different sintering temperatures. At 1250°C, the mixed oxide $PZ_{.5}T_{.5}$ specimen obtained a relative density of approximately 98.5% within eight hours.

a. Evaporation Coefficient. From the rates of fraction of liquid removed of Fig. 14a, the rate of weight loss of PbO was calculated for each temperature. Because of the one-way process of weight loss from the $PZ_{.5}T_{.5}$ sample surface, an analogy was made to the Langmuir evaporation mechanism.

Langmuir[48] postulated that the number of molecules leaving a surface is independent of the number of gas molecules striking the surface; hence, the rate of weight loss from the surface into a vacuum can be related to the equilibrium vapor pressure:

$$P_L = \frac{1}{A} \quad (dw/dt) \quad \left(\frac{2\pi RT}{M}\right)^{1/2} \qquad (3)$$

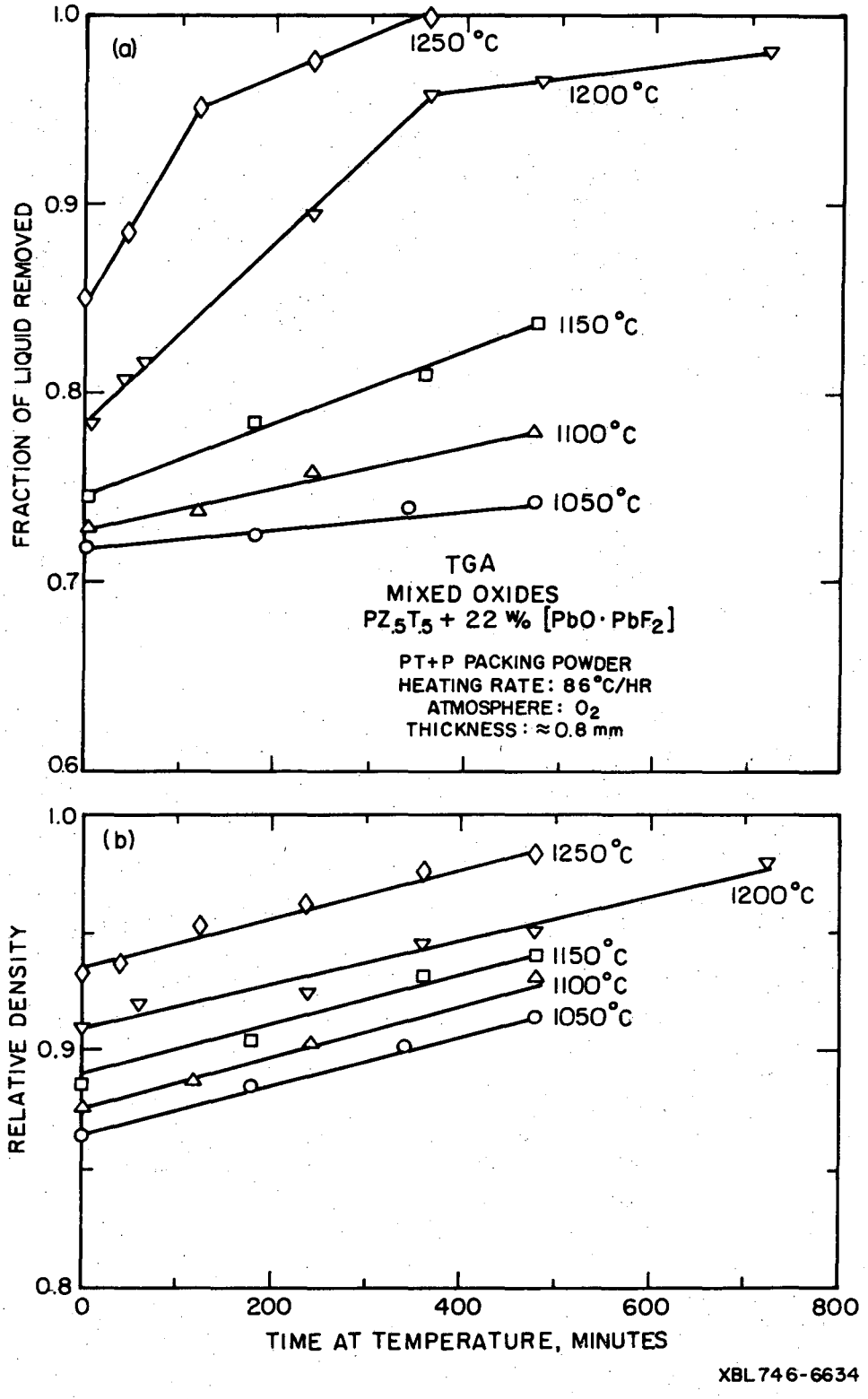

Figure 14. (a) Rate of liquid removal as a function of temperature due to a PT + P packing powder.
(b) Comparison of density after removal of the liquid at different temperatures.

where P_L is the Langmuir pressure, A is the surface area, R is the gas constant, M is the molecular weight, dw/dt is the weight loss rate, and T is the absolute temperature. If an activation energy or entropy is not involved in the evaporation process, the equilibrium vapor pressure can be determined from Eq. (3) by the Langmuir method. On the other hand, if an activation energy or entropy does exist, then the sample evaporates at a kinetically determined rate with enhanced energy or entropy barriers. The Langmuir pressure P_L would then be related to the equilibrium pressure P_{eq} by the relation:[47]

$$P_L = \alpha_v P_{eq} \tag{4}$$

where α_v is the evaporation coefficient and, in this case, is not equal to one ($\alpha_v \neq 1$). The value of P_{eq} is taken as the vapor pressure measured by the Knudsen effusion method.[30]

Although the Langmuir experiment is performed in vacuum where the walls of the vacuum system usually act as sinks for the vapor species, the weight loss studies on the $PZ_{.5}T_{.5}$ sample are similar in that the packing powder acts as a sink for the PbO molecule. From the measured rates of weight loss of PbO, the Langmuir vapor pressure, P_L, for the $PZ_{.5}T_{.5}$ specimen containing a PbO rich liquid was calculated using Eq. (3). From Knudsen effusion experiments on $PZ_{.5}T_{.5}$ + P by Holman and Fulrath,[30] a comparison of P_L with that of P_{eq} is shown in Fig. 15. The evaporation coefficient α_v is low, indicating that the evaporation of PbO from the sample involves an activation process. This is to be suspected since the evaporation rate depends on the PbO activity created by

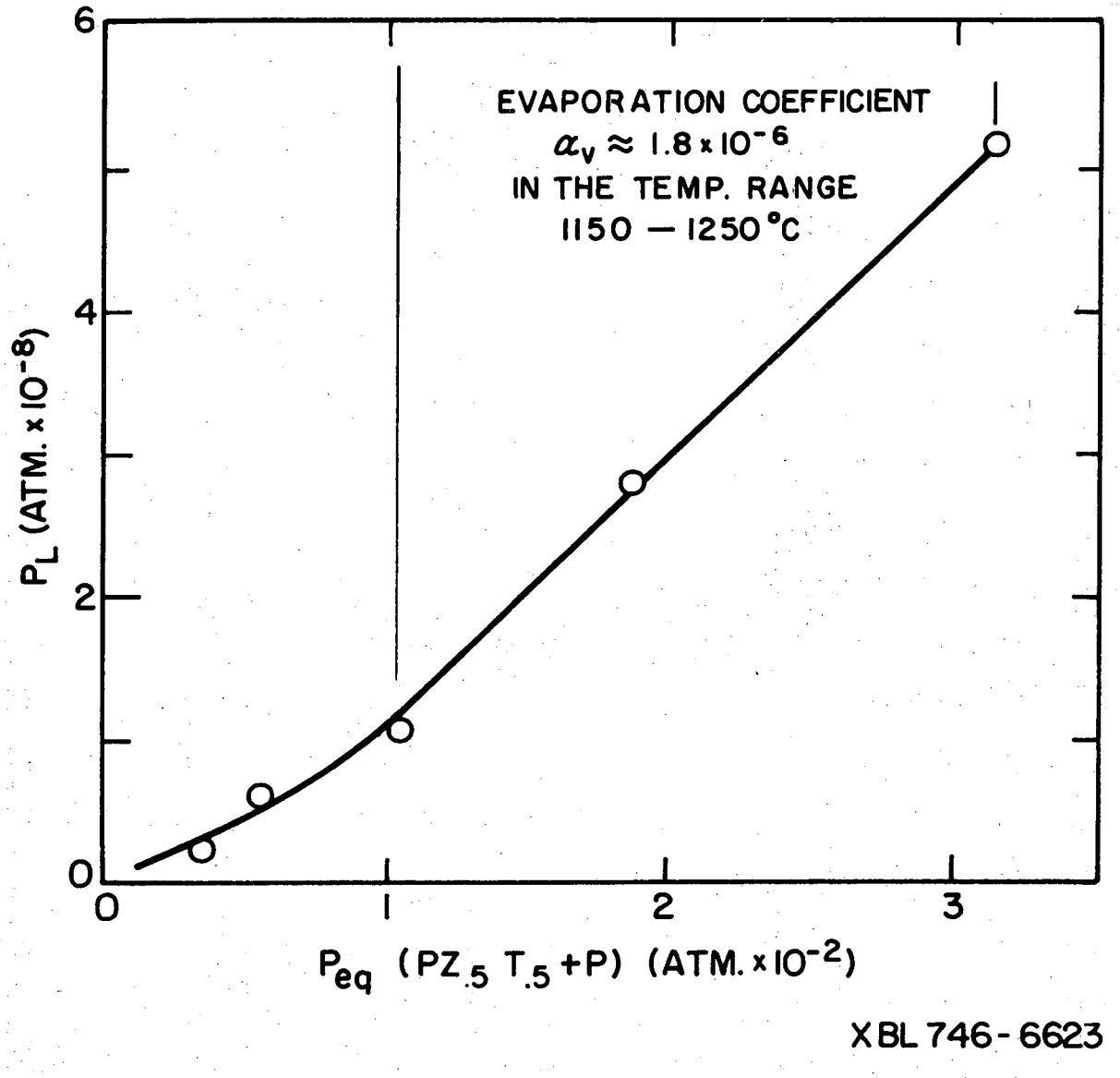

Figure 15. Determination of α_v for the evaporation of liquid PbO from $PZ_{.5}T_{.5}$ in an atmosphere of PbO activity fixed by a PT + P packing powder.

the packing powder composition. Hence, the value of α_v should vary depending on the packing powder activity of PbO, i.e., increasing for a greater PbO activity difference between packing powder and sample. It is also noted that the value of α_v appears to be constant for PbO evaporation in the temperature range from 1150° to 1250°C.

A plot of PbO vapor pressure versus 1/T for both P_L and P_{eq} (determined from Knudsen effusion data) is given in Fig. 16. The data give a higher apparent enthalpy and entropy value as compared to the apparent value obtained by Knudsen effusion. As a result, removal of a PbO molecule from the surface of the specimen requires extra energy for evaporation in an atmosphere of PbO activity set by a PT + P packing powder. It should be mentioned that these values of enthalpy and entropy are presented as apparent values in place of true values. This is because enthalpy and entropy are defined assuming a composition that is invarient with temperature, yet from the PZT phase diagram, PZT plus a rich PbO liquid does vary in composition with temperature. Hence, the apparent enthalpy and entropy values were determined and compared only to indicate the influence of an atmosphere of fixed PbO activity on the evaporation of the liquid phase.

(b) Grain Growth. During the heat treatment for sintering of a compact, the grains of the sample grow with time. The rate at which grain growth occurs is inversely proportional to the average radius of boundary curvature.[49] Because the grain size is proportional to the boundary curvature, the growth rate can be integrated to give:

$$D^2 - D_o^2 = kt$$

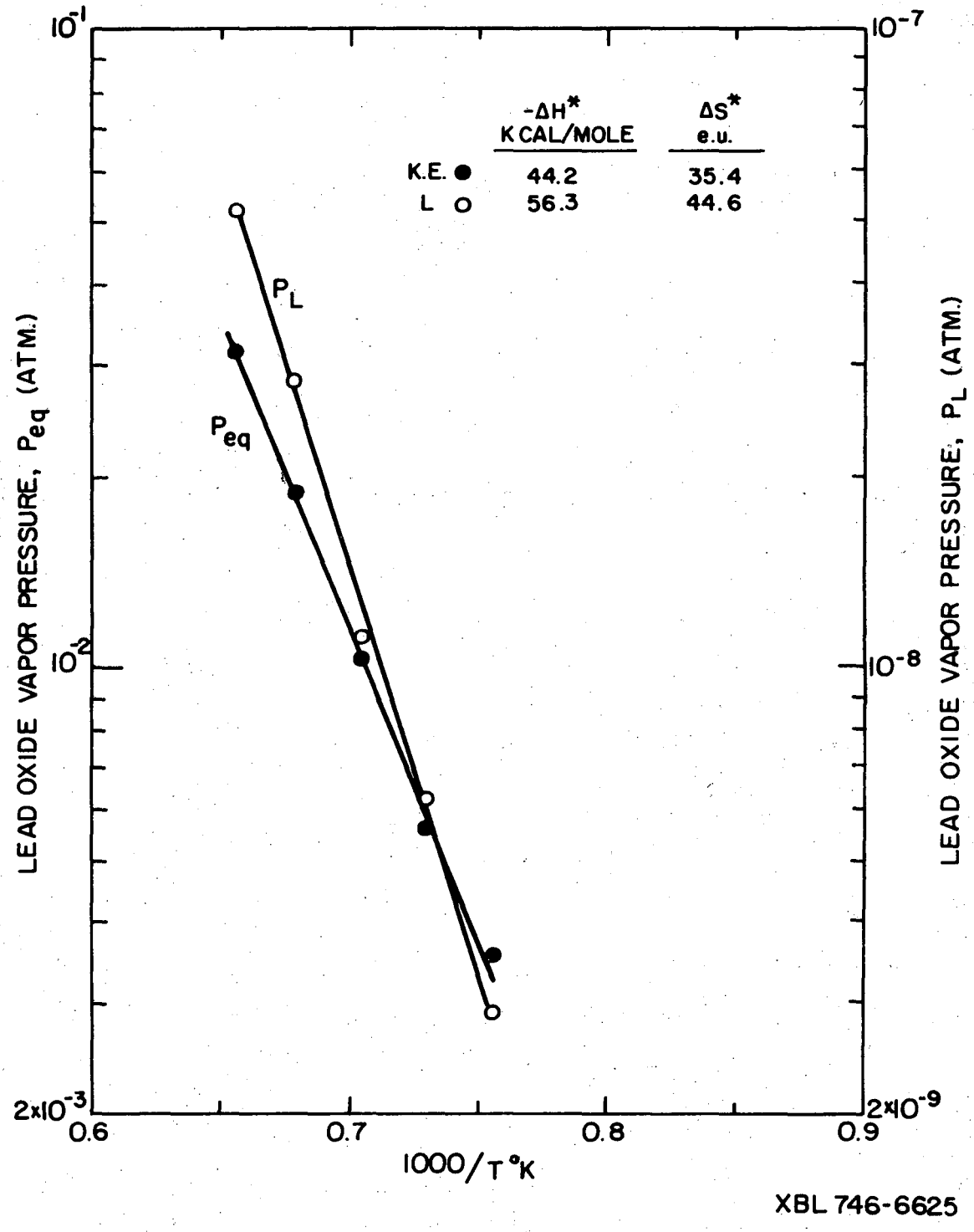

Figure 16. Lead oxide vapor pressure versus reciprocal temperature as determined by both the Langmuir equation and Knudsen effusion data.

where D is the average grain diameter,

D_o is the average grain diameter at t = o, and

k is the rate constant that depends upon the temperature and boundary mobility.

For $D_o << D$,

$$D = (kt)^{1/2}$$

It has been shown that the presence of a second phase material, including pores, can limit the rate of grain growth such that the grain size becomes proportional to the cube root of time:[50]

$$D = Kt^{1/3}$$

The grain sizes of the mixed oxide $PZ_{.5}T_{.5}$ specimens corresponding to the data of Fig. 14a at different temperatures are presented in Fig. 17. It is observed that the grains of the undoped $PZ_{.5}T_{.5}$ material can become large during sintering in a liquid phase. The time dependence of the grain size for different temperatures is indicated in Fig. 18.

A time exponent dependence of approximately 1/2 and 1/3 appears to be present in the grain growth behavior. The 1/3 slope at 1050°C is suggested to be a temperature effect where the liquid phase limits the grain boundary mobility by the degree of PZT solubility: Because grain growth involves movement of atoms across the boundary from the convex to the concave surface, the presence of the liquid phase may interfere in this process by limiting the mobility of the atom by the lower solubility at that temperature. At higher temperatures up to 1200°C, the time

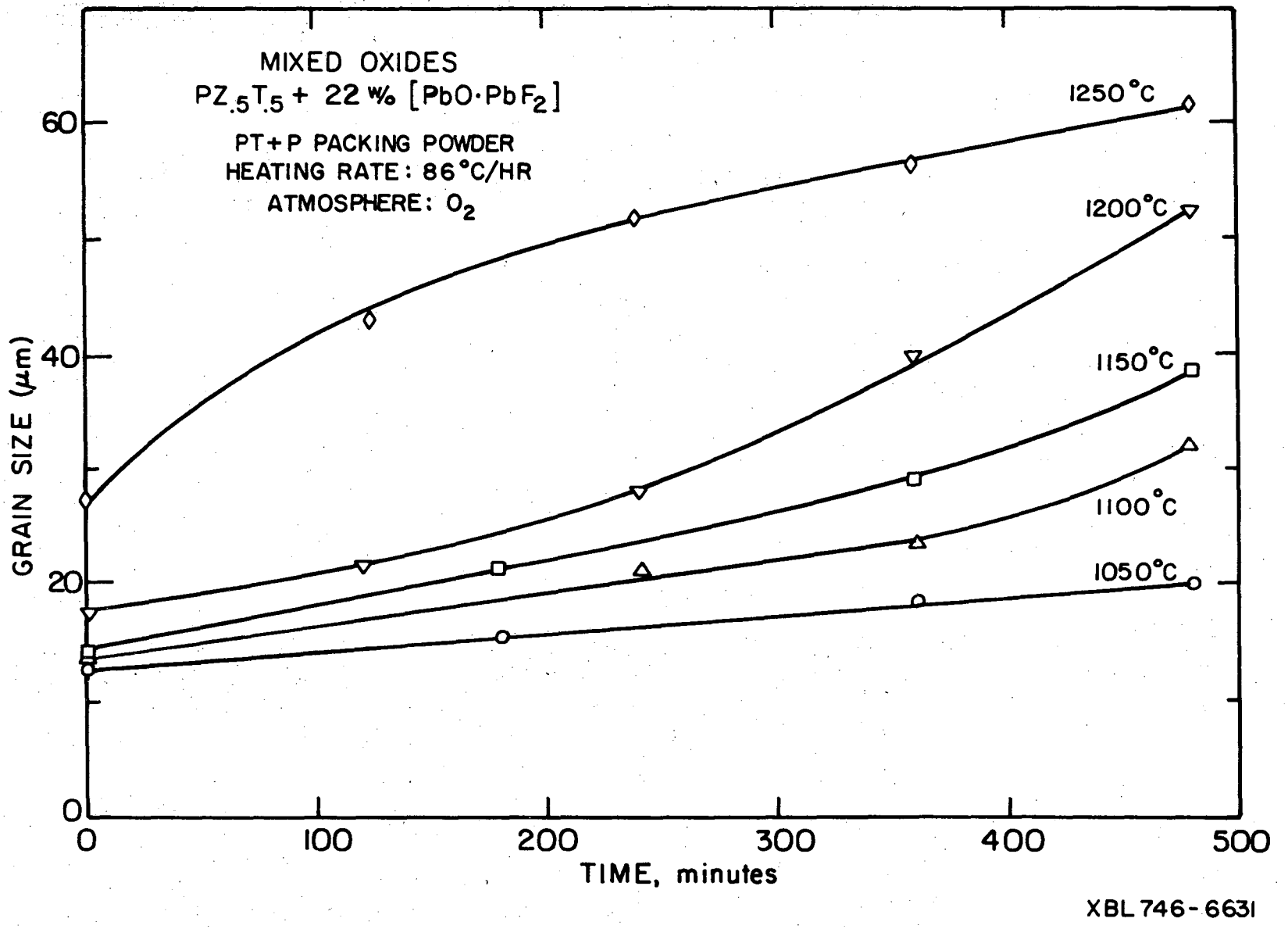

Figure 17. Grain growth data at different temperatures.

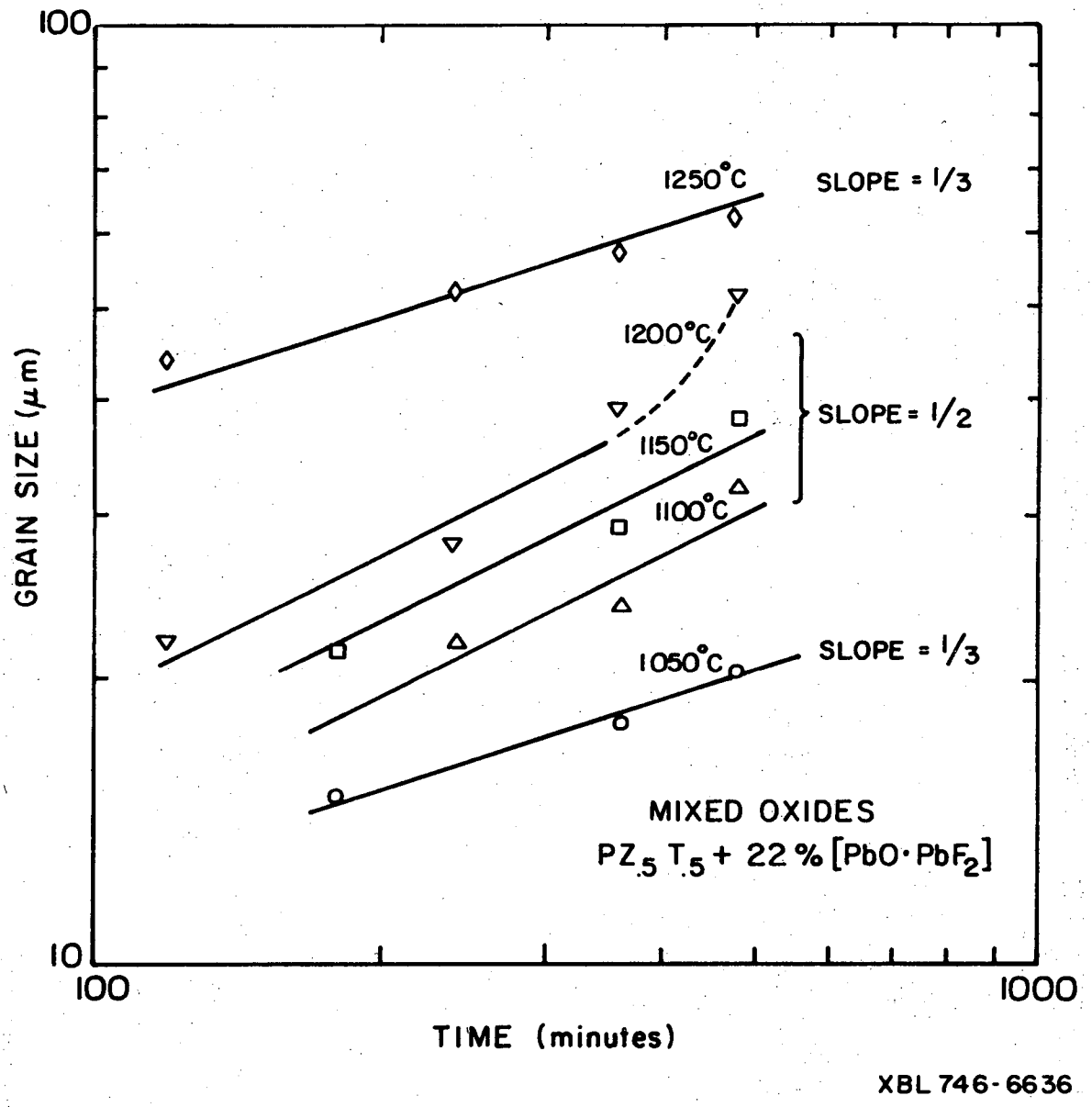

Figure 18. Grain growth data indicating the approximate time dependence at different temperatures.

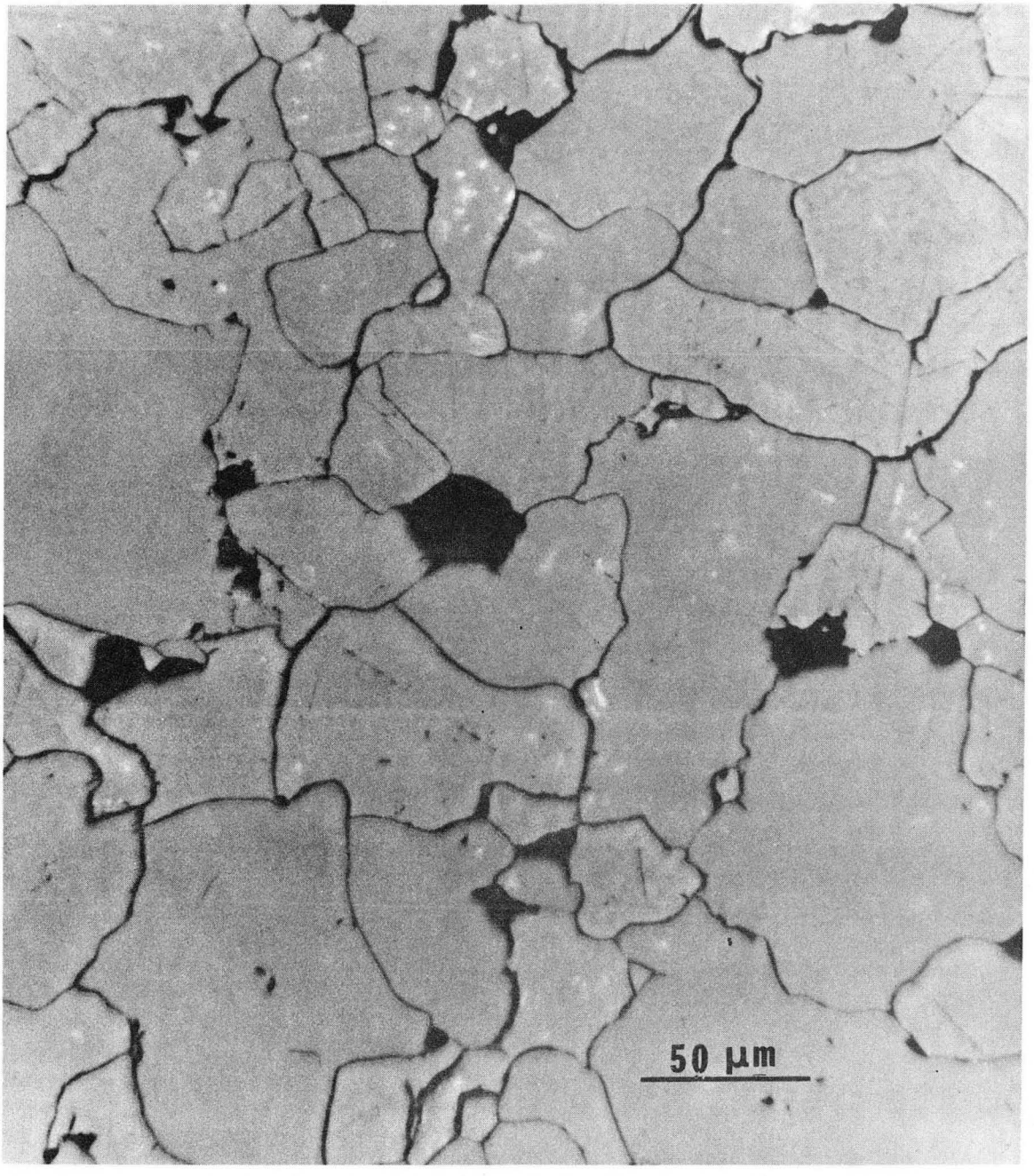

XBB 746-4292

Figure 19. Photomicrograph of a mixed oxide prepared $PZ_{.5}T_{.5}$ sample heat treated at 1250°C for 8 hrs in a PT + P packing powder.

dependence exponent appears to become 1/2. In this case, the temperature is high enough that the grain boundary mobility is not limited by solubility in the liquid phase and the rate of grain growth can proceed in a manner inversely proportional to the radius of curvature. The dash extension at 1200°C is thought to be the beginning of exaggerated grain growth. At a temperature of 1250°C, the grain size once again appears to have a time exponent dependence of 1/3. Since most of the liquid is removed at this temperature and the relative density is high enough to develop a closed pore condition, the exponent of 1/3 may result from the decrease in grain boundary mobility due to the reduced amount of liquid phase that now may be in pockets along the grain boundary.

A photomicrograph of the microstructure of a mixed oxide sample heated at 1250°C for eight hours is shown in Fig. 19. The large dark areas of the microstructure are attributed to "pull-outs" of individual grains during polishing. Although the grain size becomes large in unmodified $PZ_{.5}T_{.5}$ from sintering in the presence of a liquid phase, this effect may be overcome by the addition of dopants that could help inhibit grain growth.

E. Chemically Prepared $PZ_{.5}T_{.5}$

The chemically prepared $PZ_{.5}T_{.5}$ material containing the optimum $PbO \cdot PbF_2$ content was liquid phase sintered in a PT + P packing powder composition to investigate the effect of temperature on removal of the liquid. Figure 20 shows the fraction of liquid removed (determined by the TG method) versus temperature. Because of the lower weight percent of liquid in the chemically prepared $PZ_{.5}T_{.5}$ after hot pressing, as compared to the mixed oxide material, most of the liquid was removed from

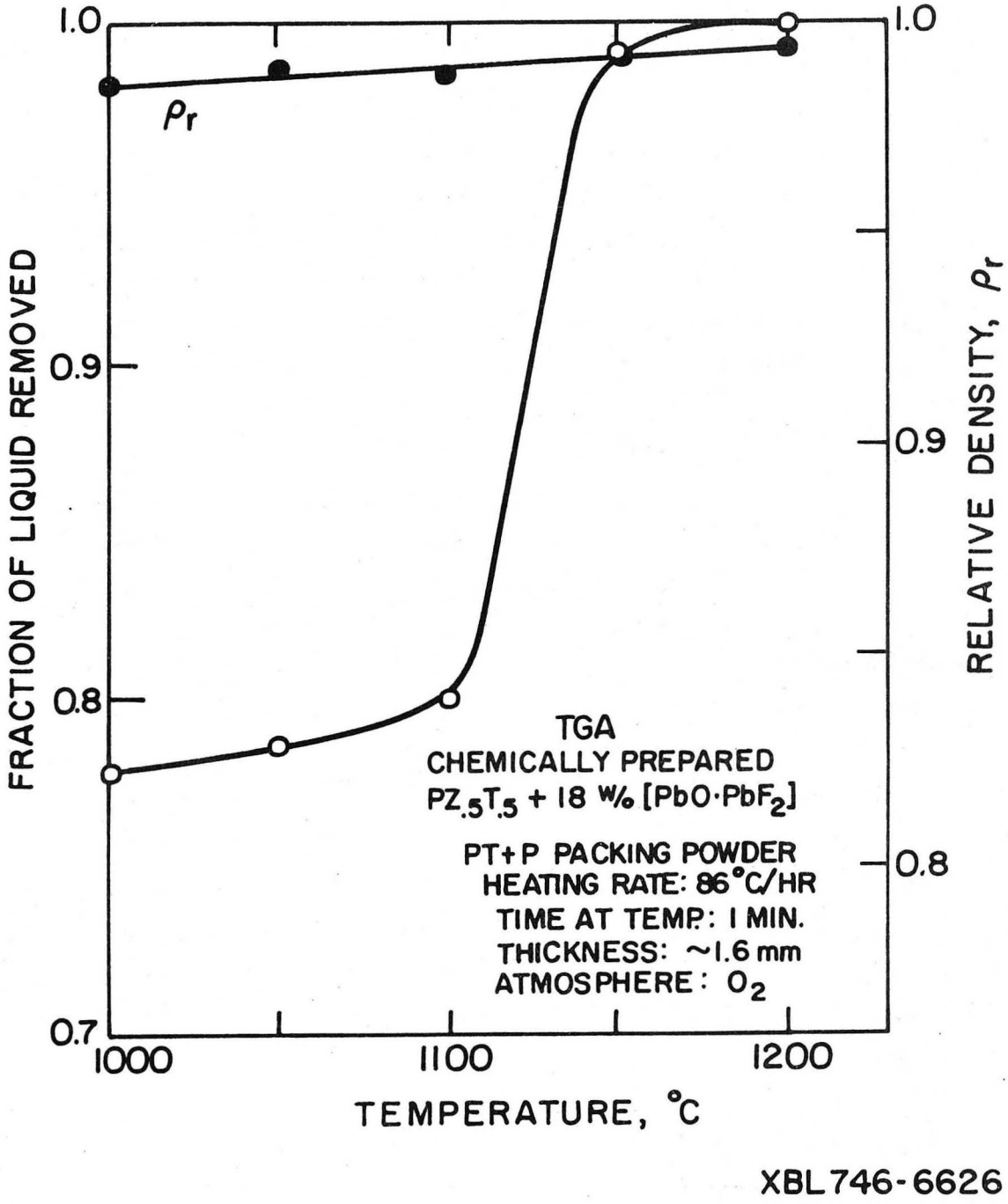

Figure 20. Fraction of liquid removed and corresponding relative density as a function of temperature.

the specimen by heating up to a temperature above 1100°C. Also, the relative density continuously increased with temperature indicating that by heating up the chemically prepared specimen to a temperature of 1200°C the relative density can reach a value of 99.5%. This represents the highest of the reported values of density for an unmodified PZT material.

Figure 21 gives the increase in grain size of the material at reaching temperature. A photomicrograph of the chemically prepared specimen heated up to 1200°C and held for one min. is shown in Fig. 22. The microstructure appears rather uniform for an undoped PZT material.

F. Ferroelectric and Piezoelectric Properties

Specimens of $PZ_{.5}T_{.5}$ prepared from mixed oxides were densified at 1250°C for eight hours by the liquid phase densification technique. To determine the ferroelectric and piezoelectric behavior of $PZ_{.5}T_{.5}$ due to intrinsic nonstoichiometric changes in composition, a subsequent heat treatment was performed in various packing powder compositions of PbO activity that allowed the sample to remain within its single phase region. The packing powder compositions chosen were $PZ_{.5}T_{.5}$ + P (high PbO activity side of the single phase region), $PZ_{.2}T_{.8}$ + P, PT + P, PZ + Z, $PZ_{.8}T_{.2}$ + T, and $PZ_{.5}T_{.5}$ + Z + T (low PbO activity side of the single phase width). The specimens had a thickness of 0.4 mm and were fired at 1100°C for 24 hours in the different multi-phase packing powder compositions. The heat treatment for 24 hours was an attempt to equilibrate the PbO activity of the specimen with that of the activity of PbO set by the packing powder. It has been shown that a porous PZT compact whose composition is set on the high PbO activity side of its single phase width can equilibrate in 12 hours at 1100°C with a packing powder

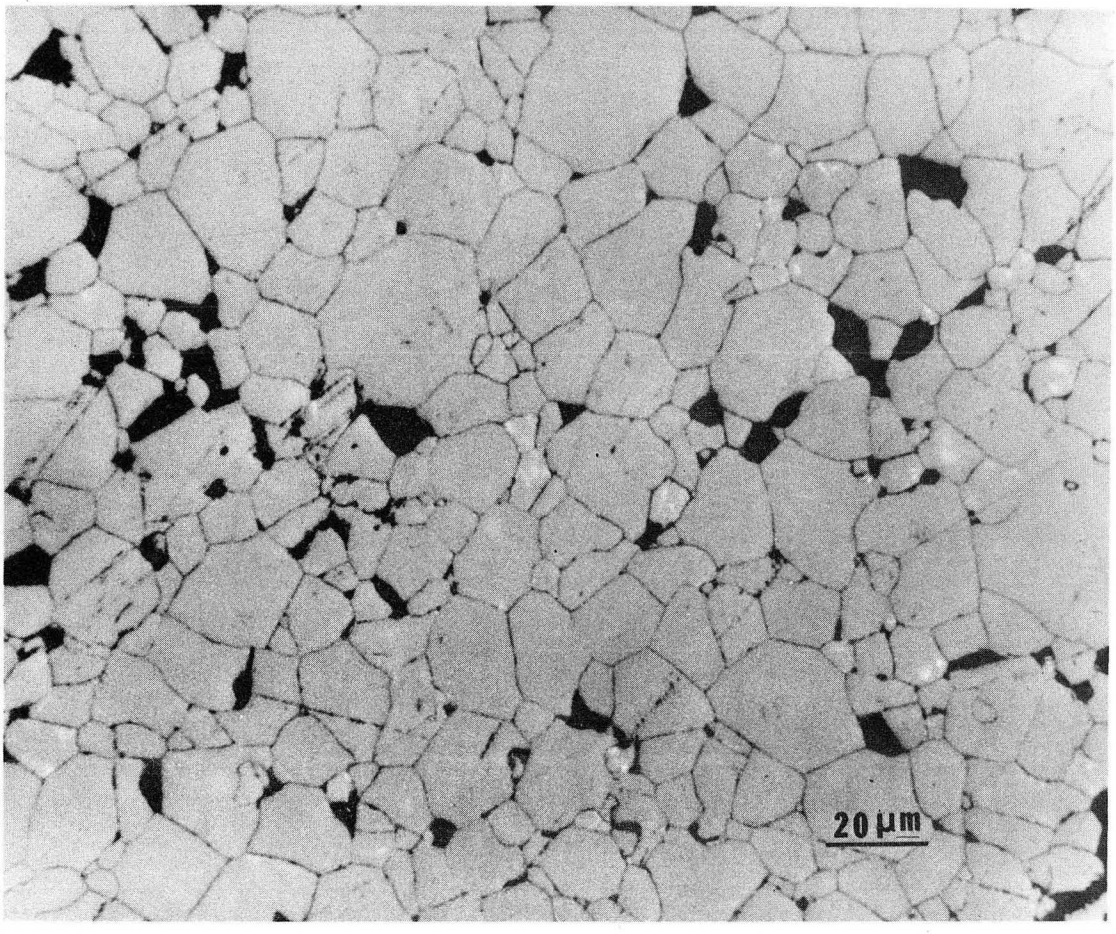

500×

XBB 746-4291

Figure 22. Photomicrograph of the chemically prepared $PZ_{.5}T_{.5}$ material heat treated for Imin at 1200°C.

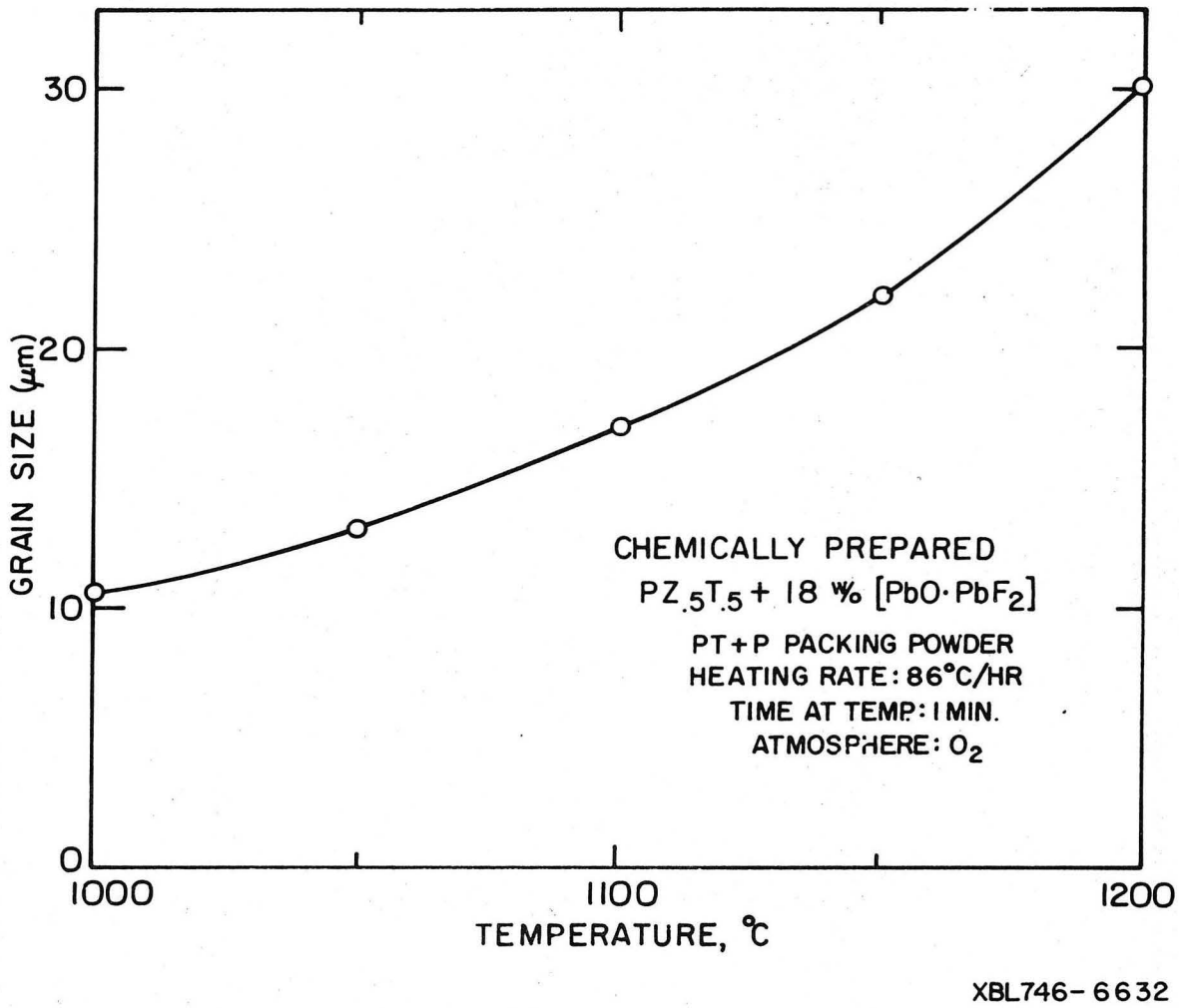

Figure 21. Grain size versus temperature for the chemically prepared $PZ_{.5}T_{.5}$ material.

composition on the other side of the single phase width.[29] Based on this information, it was assumed that a dense specimen having an intrinsic nonstoichiometric composition, set by a PT + P packing powder, would equilibrate at 1100°C in 24 hours with a PbO activity within its single phase region as set by the other packing powder compositions.

The values of the ferroelectric and piezoelectric parameters measured on the $PZ_{.5}T_{.5}$ specimens with respect to the packing powder used to establish a PbO atmosphere are given in Table III. Parameter definition and relations are presented in the Appendix. The measured values of the ferroelectric parameters P_m, E_c, and P_r are reproduced in Fig. 23 versus the lead oxide defective mole fraction, X_{PbO}, as set at 1100°C by the different packing powder compositions. Basically there is very little difference in the parameters with X_{PbO}, except at the boundaries of the single phase width and at $X_{PbO} = 0.02$ set by the PZ + Z composition. This is more readily observed by examining the ferroelectric hysteresis loops as shown in Fig. 24.

At $X_{PbO} = 0$, the broad hysteresis loop is probably due to the lack of lead vacancies to help promote domain switching; hence, a large E_c value along with a low P_m. At $X_{PbO} = 0.025$, on the other side of the single phase width, it has been reported that both a rhombohedral and a tetragonal crystal structure may exist.[30] The relative low E_c and P_r values may therefore reflect the ease of domain movement due to the mixed crystal structure since the rhombohedral lattice has eight possible directions of polarization as compared to six directions in the tetragonal lattice. This is in spite of the large increase in oxygen vacancies which have been shown to hinder domain motion.

Table III

PACKING POWDER X_{PbO} AT 1100°C	P_r $\frac{\mu coul.}{cm^2}$	P_m $\frac{\mu coul.}{cm^2}$	E_c $\frac{kv}{cm}$	K_{33}^T $\frac{\epsilon_{33}^T}{\epsilon_o}$ *	s_{11}^E $\frac{10^{-12}m^2}{newton}$	s_{11}^D $\frac{10^{-12}m^2}{newton}$	k_p	k_{31}	d_p $\frac{10^{-12}coul}{newton}$	d_{31} $\frac{10^{-12}coul}{newton}$	g_p $\frac{10^{-3}vm}{newton}$	g_{31} $\frac{10^{-3}vm}{newton}$
$PZ_{.5}T_{.5}$+P X = 0	10.6	13.4	14.0	613	9.1	8.3	0.486	0.292	196	91.8	36.1	16.9
$PZ_{.2}T_{.8}$+P X=0.007	8.9	15.6	9.0	609	9.0	8.3	0.476	0.286	196	89.4	36.4	16.6
PT+P X =0.011	8.2	15.3	9.6	545	9.1	8.4	0.476	0.286	150	85.0	31.1	17.6
PZ+Z X =0.020	12.7	16.3	11.6	512	9.2	8.4	0.476	0.286	150	82.5	33.1	18.2
$PZ_{.8}T_{.2}$+Z+T X=0.023	10.0	15.3	10.9	564	9.2	8.5	0.475	0.285	230	86.8	46.0	17.3
$PZ_{.5}T_{.5}$+Z+T X=0.025	8.3	15.1	7.9	568	9.2	8.5	0.476	0.286	350	87.2	69.6	17.3

* MEASURED AT 1 KHz AND $\epsilon_o = 8.85 \times 10^{-12}$ farad/m

XBL 746-6619

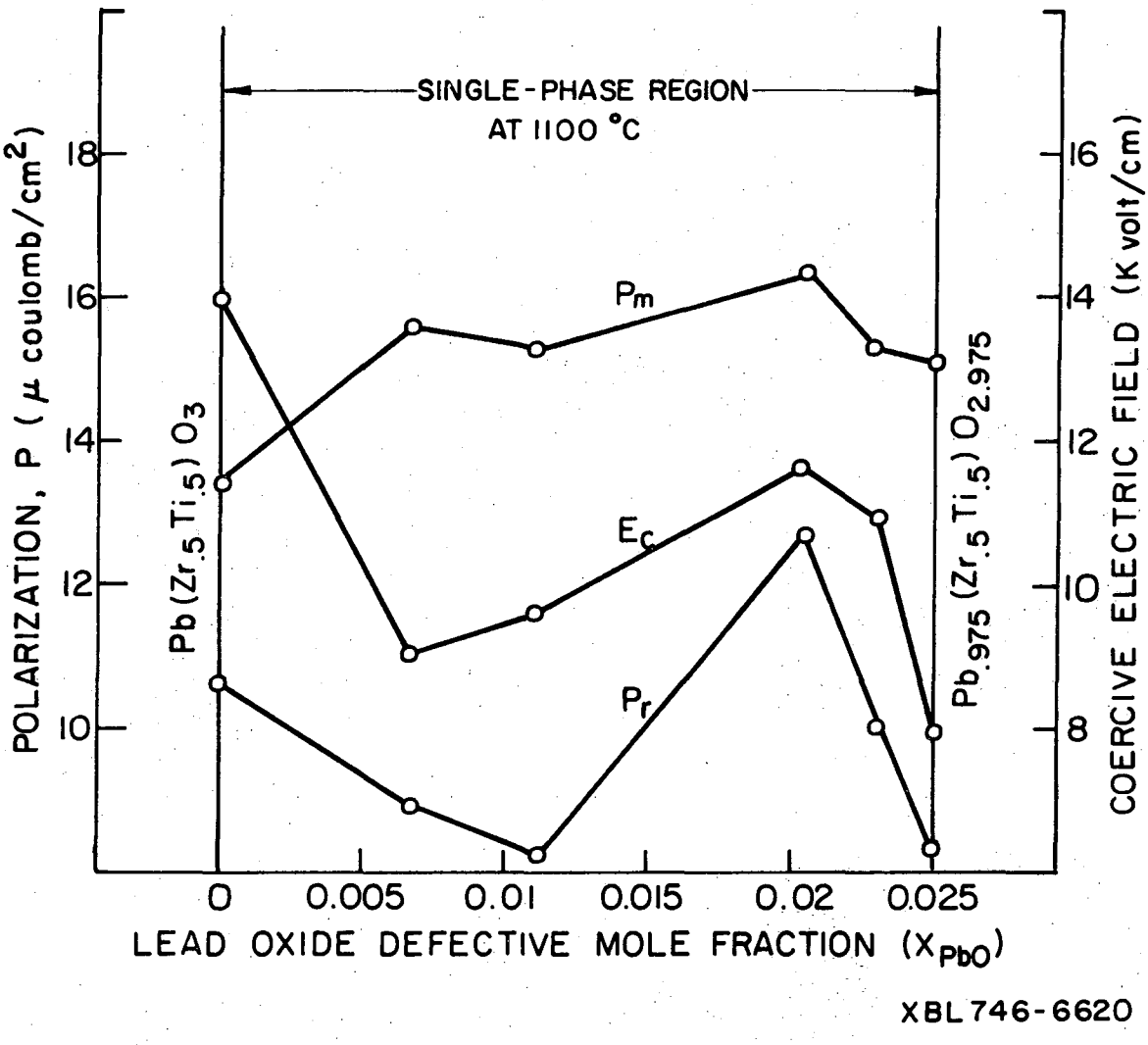

Figure 23. Ferroelectric parameters as a function of the lead oxide defective mole fraction as set by the different packing powder compositions at 1100°C.

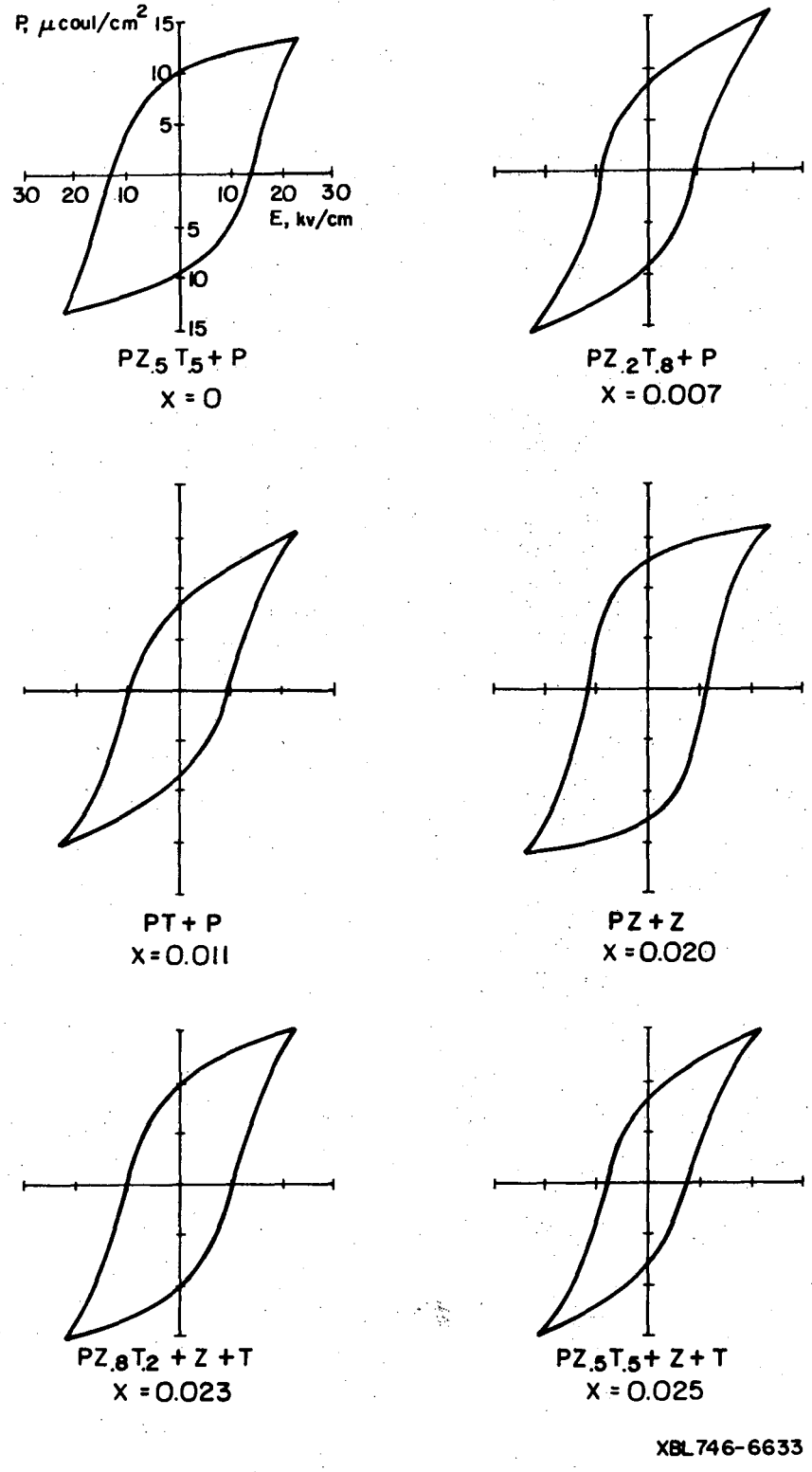

Figure 24. Ferroelectric hysteresis loops of $PZ_{.5}T_{.5}$ where x equals the lead oxide defective mole fraction at 1100°C.

For the PZ + Z packing powder composition, the hysteresis loop of $PZ_{.5}T_{.5}$ seems to have more of a square loop shape with higher P_m, E_c, and P_r values. Assuming that the specimen has equilibrated with the PbO activity of PZ + Z, it appears that the ferroelectric behavior can be slightly influenced by the intrinsic lead and oxygen vacancy concentration.

Figures 25 and 26 reproduce the values of the dielectric constant and the piezoelectric parameters with X_{PbO}, indicating no change in k_p, k_{31}, d_{31}, and g_{31}, and only a small change in dielectric constant. The high value of d_p at $X_{PbO} = 0.025$ is probably due once again to the ease of domain movement in a mixed rhombohedral and tetragonal crystal structure.

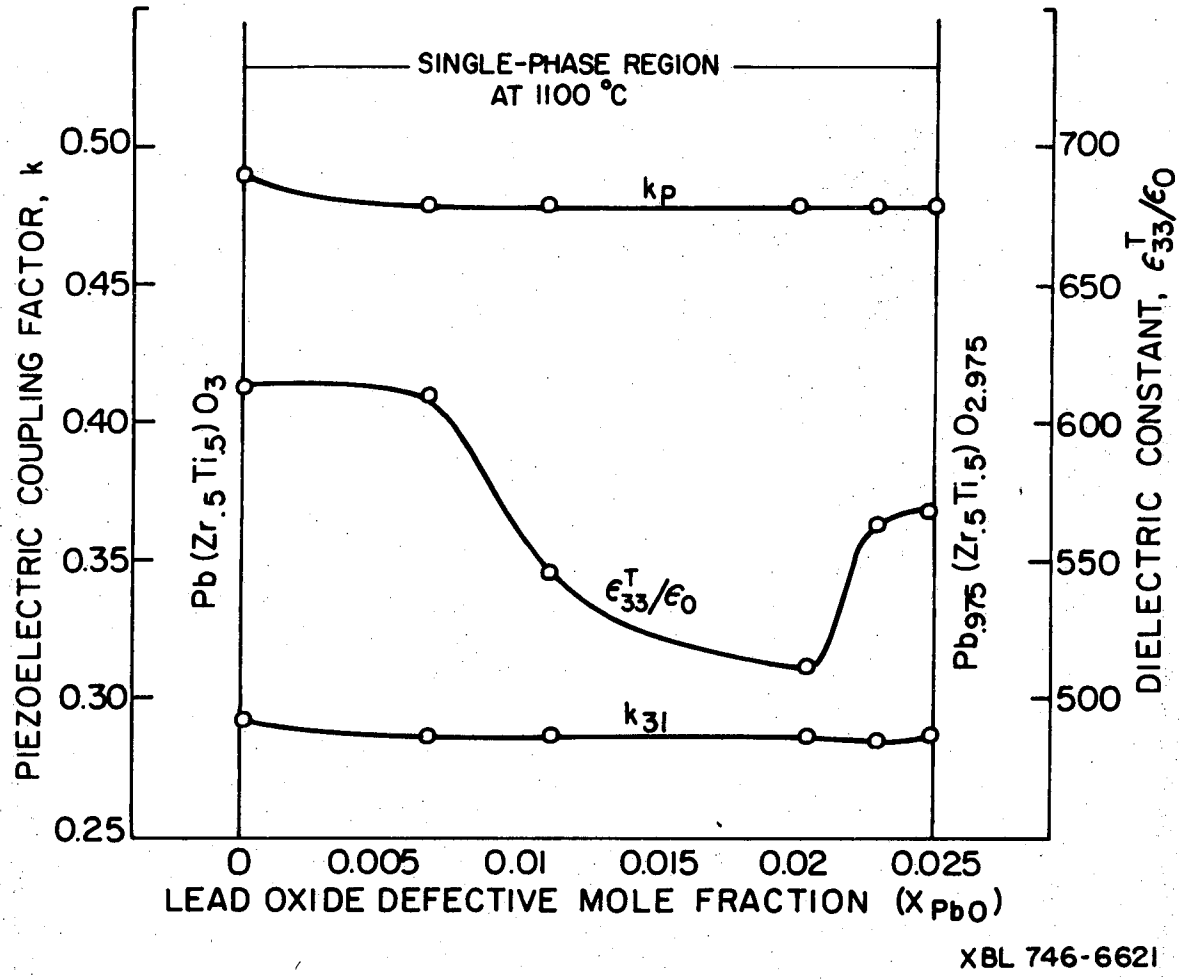

Figure 25. Piezoelectric parameter data versus lead oxide defective mole fraction at 1100°C.

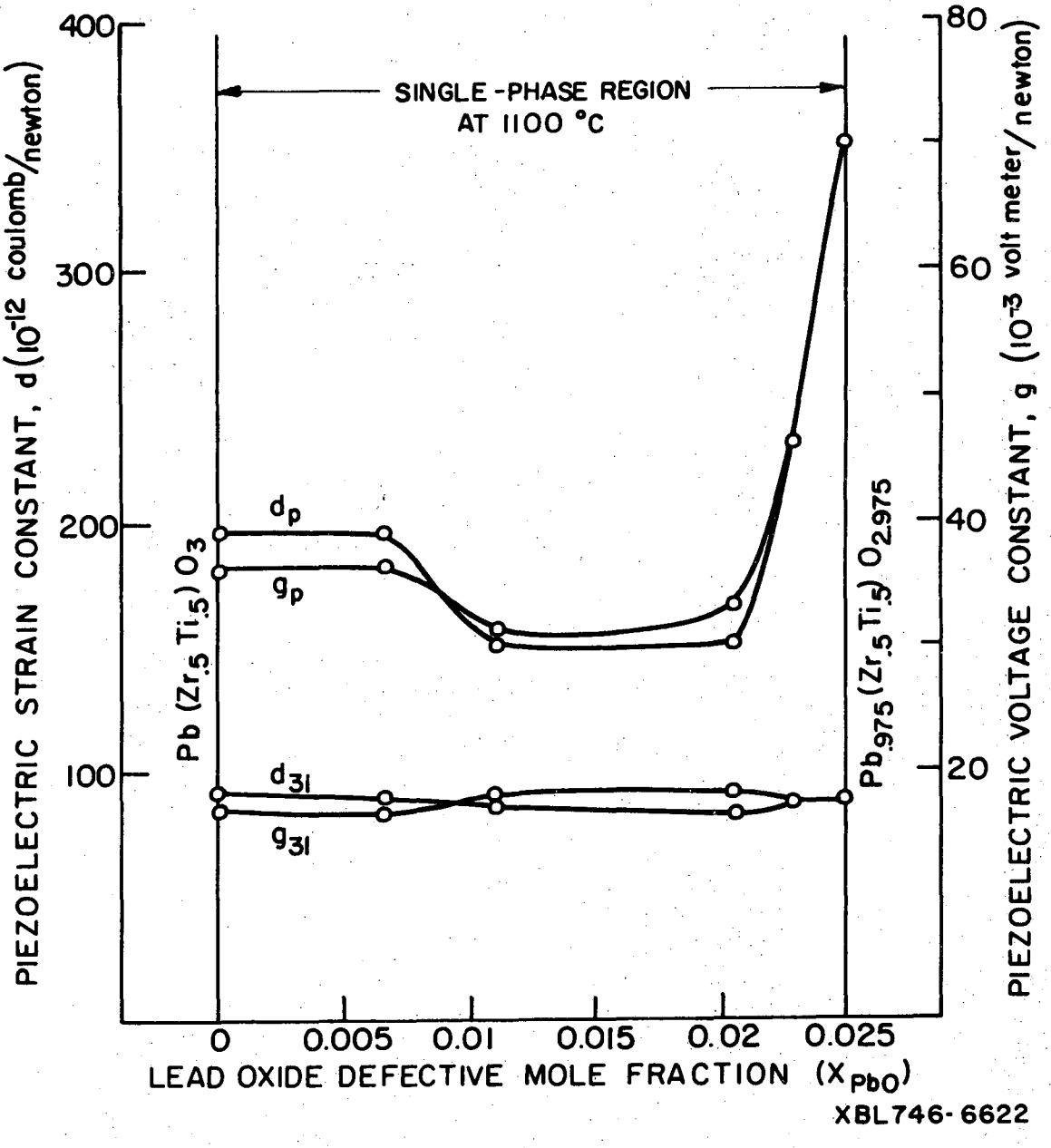

Figure 26. Piezoelectric parameter data versus lead oxide defective mole fraction at 1100°C.

IV. SUMMARY AND CONCLUSIONS

By the use of a combination of conventional processing methods, a unique liquid phase densification technique was developed for the lead zirconate titanate system. The densification procedure is essentially a two-step process:

(1) Use of a low temperature liquid phase to optimize, with the aid of applied pressure, the rearrangement process of a PZT compact upon formation of the liquid.

(2) A subsequent heat treatment, without applied pressure, to provide liquid phase sintering within a fixed PbO atmosphere that permits the liquid to be removed from the PZT sample in a controlled manner, yet maintain the PZT within its single phase region.

The addition of $PbO \cdot PbF_2$ to both the mixed oxides and chemically prepared $PZ_{.5}T_{.5}$ materials to form a low temperature liquid phase allowed enhanced sintering to occur by the liquid phase densification technique. A relative density as high as 99.5% was easily obtained for an unmodified $PZ_{.5}T_{.5}$ that was chemically prepared and heated at a rate of 86°C/hr to 1200°C and held for one min. in a PT + P packing powder composition.

Establishing a fixed PbO vapor pressure from a multiphase packing powder composition within the PZT system permitted controlled removal of the PbO portion of the liquid from the sample, leaving the PbF_2 to evaporate freely. The rate of removal of the PbO-rich liquid depends on the PbO activity difference between the packing powder composition and the $PZ_{.5}T_{.5}$ sample; decreasing the activity difference reduces the rate of PbO evaporation. As a result, evaporation of the liquid from the

sample involves an activation process as indicated by the low evaporation coefficient determined from evaporation in a PT + P packing powder.

For the range of sample thickness investigated, the rate of removal of the liquid is independent of thickness if:

(1) The sample is liquid phase sintered in an atmosphere of PbO where the reaction rate of PbO evaporation at the surface of the sample is the rate controlling process.

(2) The sample during liquid phase sintering has not reached a density where a closed pore condition develops.

Otherwise, the rate of liquid removal becomes sample thickness dependent.

Although the rate of grain growth appears to behave within the accepted values of the time exponent, the grain size of unmodified $PZ_{.5}T_{.5}$ becomes large from sintering in a liquid derived from $PbO \cdot PbF_2$. For the chemically prepared $PZ_{.5}T_{.5}$, the grain size was smaller and the microstructure appeared to be more uniform than the mixed oxides material.

By proper choice of multiphase packing powder composition, it is possible to fix the intrinsic nonstoichiometry of $PZ_{.5}T_{.5}$ across its single phase width. On this basis, an attempt was made to establish sample equilibrium with various multiphase packing powder compositions to determine the effect of the ferroelectric and piezoelectric properties on the intrinsic nonstoichiometry of $PZ_{.5}T_{.5}$. The results indicated only secondary effects, except perhaps in the planar piezoelectric strain constant which increased at the PbO deficient side of the single phase width.

Results of the liquid phase densification technique indicate that a highly dense, unmodified single phase $PZ_{.5}T_{.5}$ ceramic of small thickness can be produced having a fixed stoichiometry. To obtain dense samples of greater thickness, by this technique, would require further investigation. Yet, because the basic principles of the processing procedure should not change, it is assumed that thicker samples of composition within the PZT system can be obtained by this densification technique.

ACKNOWLEDGMENTS

The author wishes to thank Professor Richard M. Fulrath for his continued support, advice, and encouragement through the course of this work. Additional appreciation is expressed to Professor Joseph A. Pask and Professor Michael C. Williams for their helpful comments, suggestions, and editing of the thesis.

I am also grateful to Dr. Gautam Bandyopadhyay, Dr. Leo Froschauer, Dr. Robert L. Holman, and Dipak R. Biswas, for their interest and enlightening discussions. Further thanks are extended to Jack Wodei, Walt Toutolmin, Gloria Pelatowski, and Kelly Radmilovic, for their excellent experimental assistance.

This work was carried out under the auspices of the United States Atomic Energy Commission.

REFERENCES

1. D. A. Berlincourt, C. Cmolik, and H. Jaffe, "Piezoelectric Properties of Polycrystalline Lead Titanate Zirconate Compositions," Proc. IRE 48 [2] 220-229 (1960).

2. B. Jaffe, R. S. Roth, and S. Marzullo, "Properties of Piezoelectric Ceramics in the Solid-Solution Series Lead Titanate-Lead Zirconate-Lead Oxide: Tin Oxide and Lead Titanate-Lead Hafnate," J. Res. Natl. Bur. Standards, 55 [5] 239-254 (1955).

3. F. Kulcsar, "Electromechanical Properties of Lead Titanate Zirconate Ceramics with Lead Partially Replaced by Calcium or Strontium," J. Am. Ceram. Soc., 42 [1] 49-51 (1959).

4. F. Kulcsar, "Electromechanical Properties of Lead Titanate Zirconate Ceramics modified with Certain Three or Five-Valent Additions," J. Am. Ceram. Soc., 42 [7] 343-349 (1959).

5. B. Jaffe, R. S. Roth, and S. Marzullo, "Piezoelectric Properties of Lead Zirconate-Lead Titanate Solid-Solution Ceramic Ware," J. Appl. Phys., 25 809-810 (1954).

6. R. Gerson, "Variation in Ferroelectric Characteristics of Lead Zirconate Titanate Ceramics Due to Minor Chemical Modifications," J. Appl. Phys., 31 [1] 188-194 (1960).

7. K. Okazaki and K. Nagata, "Effects of the Density and the Grain Size of Piezoelectric Ceramics Influencing Upon the Electrical Properties," Trans. Inst. Electronics and Communication of Japan, 53-C [11] 815-822 (1970).

8. K. Okazaki and K. Nagata, "Effects of the Density and the Grain Size of $Pb(Zr-Ti)O_3$ Ceramics Influencing Upon the Elastic and Piezoelectric Properties," presented at the International Conference on Mechanical Behavior of Materials, Kyoto, Japan, August 1971.

9. G. H. Haertling, "Hot-Pressed Lead Zirconate-Lead Titanate Ceramics Containing Bismuth," Am. Ceram. Soc. Bull., 43 [12] 875-879 (1964).

10. G. H. Haertling and C. E. Land, "Hot-Pressed $(Pb,La)(Zr,Ti)O_3$ Ferroelectric Ceramics for Electro-optic Applications," J. Am. Ceram. Soc., 54 [1] 1-11 (1971).

11. K. Okazaki and K. Nagata, "Effects of Grain Size and Porosity on Electrical and Optical Properties of PLZT Ceramics," J. Am. Ceram. Soc., 56 [2] 82-86 (1973).

12. G. H. Haertling, "Improved Hot-Pressed Electro-optic Ceramics in the $(Pb,La)(Zr,Ti)O_3$ System," J. Am. Ceram. Soc., 54 [6] 303-309 (1971).

13. C. E. Land and P. D. Thacher, "Ferroelectric Ceramic Electro-optic Materials and Devices," Proc. IEEE Trans. Electron Devices, 57 [5] 751-768 (1969).

14. P. D. Thacher and C. E. Land, "Ferroelectric Electro-optic Ceramics with Reduced Scattering," IEEE Trans. Electron Devices, 16 [6] 512-521 (1969).

15. D. A. Northrop, "Vaporization of Lead Zirconate-Titanate Materials," J. Am. Ceram. Soc., I 50 [9] 441-445 (1967); II 51 [7] 357-361 (1968).

16. S. Fushimi and T. Ikeda, "Phase Equilibrium in the System $PbO-TiO_2-ZrO_2$," J. Am. Ceram. Soc., 50 [3] 129-132 (1967).

17. K. Nagase and T. Nitta, "Evaporation from $Pb(Ti_{1-x}Zr_x)O_3$ Compositions on Firing," Metsushita Elect. Ind. Co., National Tech. Report 10, [2] 162-169 (1964).

18. R. L. Moon, "High Temperature Phase Equilibra in the Lead Titanate-Lead Zirconate System," Ph.D. Thesis, Univ. of Calif. Berkeley, 1967 (UCRL 17545).

19. P. D. Levett, "Factors Affecting Lead Zirconate-Lead Titanate Ceramics," Am. Ceram. Soc. Bull., 42 [6] 348-352 (1963).

20. A. H. Webster, T. B. Weston and N. F. H. Bright, "Effect of PbO Deficiency on the Piezoelectric Properties of Lead Zirconate-Titanate Ceramics," J. Am. Ceram. Soc., 50 [9] 490-1 (1967).

21. R. B. Atkin and R. M. Fulrath, "Point Defects and Sintering of Lead Zirconate-Titanate," J. Am. Ceram. Soc., 54 [5] 265-270 (1971).

22. W. K. Kingery and M. Berg, "Study of the Initial Stages of Sintering Solids by Viscous Flow, Evaporation-Condensation, and Self-Diffusion," J. Appl. Phys., 26 [10] 205-212 (1955).

23. R. L. Coble, "Sintering Crystalline Solids, I. Intermediate and Final Stage Diffusion Models," J. Appl. Phys., 32 [5] 787-792 (1961).

24. R. L. Coble and T. K. Gupta, "Intermediate Stage Sintering," in Sintering and Related Phenomena, edited by Kuczynski, Hooten, and Gibbon, Gordon and Breach Science Publishers, New York (1967).

25. B. Jaffe, W. R. Cook, Jr., and H. Jaffe, Piezoelectric Ceramics, Chapt. 7: "Solid Solution of $Pb(Ti, Zr, Sn, Hf)O_3$," pp. 135-183, Academic Press Inc., New York (1971).

26. R. H. Dungan, H. M. Barnett and A. H. Stark, "Phase Relations and Electrical Parameters in the Ferroelectric-Antiferroelectric Region

of the System $PbZrO_3$-$PbTiO_3$-$PbNb_2O_6$," J. Am. Ceram. Soc., 45 [8] 382-388 (1962).

27. G. S. Snow, "Fabrication of Transparent Electro-optic PLZT Ceramics by Atmosphere Sintering," J. Am. Ceram. Soc., 56 [2] 91-96 (1973).

28. K. H. Hardtl and H. Rav, "PbO Vapour Pressure in the $Pb(Ti_{1-x}Zr_x)O_3$ System," Solid State Commun., 7 [1] 41-45 (1969).

29. R. L. Holman and R. M. Fulrath, "Intrinsic Nonstoichiometry in Single-Phase $Pb(Zr_{0.5}Ti_{0.5})O_3$," J. Am. Ceram. Soc., 55 [4] 192-195 (1972).

30. R. L. Holman and R. M. Fulrath, "Intrinsic Nonstoichiometry in the Lead Zirconate-Lead Titanate System Determined by Knudsen Effusion," J. Appl. Phys., 44 [12] 5227-5236 (1973).

31. G. H. Haertling, "Grain Growth and Densification of Hot-Pressed Lead Zirconate-Lead Titanate Ceramics Containing Bismuth," J. Am. Ceram. Soc., 49 [3] 113-118 (1966).

32. W. D. Kingery, "Sintering in the Presence of a Liquid Phase," in Ceramic Fabrication Processes, Edited by W. D. Kingery, the M.I.T. Press., Cambridge, Mass. (1958).

33. W. D. Kingery, "Densification During Sintering in the Presence of a Liquid Phase. I. Theory," J. Appl. Phys., 30 301-306 (1959).

34. R. B. Atkin, "Sintering and Ferroelectric Properties of Lead Zirconate Titanate Ceramics," D. Eng. Thesis, Univ. of Calif. Berkeley, 1970 (UCRL-20309).

35. L. M. Brown and K. S. Mazdiyasni, "Cold-Pressing and Low-Temperature Sintering of Alkoxy-Derived PLZT," J. Am. Ceram. Soc., 55 [11] 541-547 (1972).

36. G. S. Snow, "Improvements in Atmosphere Sintering of Transparent PLZT Ceramics," J. Am. Ceram. Soc., 56 [9] 479-480 (1973).

37. G. H. Haertling and C. E. Land, "Recent Improvements in the Optical and Electro-optic Properties of PLZT Ceramics," Ferroelectrics, 3 [2,3,4] 269-280 (1972).

38. R. L. Fullman, "Measurement of Particle Size in Opaque Bodies," Trans. AIME, 197 [3] 447-452 (1953).

39. S. Fushimi and T. Ikeda, "Single Crystals of Lead Zirconate-Titanate Solid Solutions," Japan J. Appl. Phys., 3 171-172 (1964).

40. K. Tsuzuki, K. Sakata, S. Hasegawa, and G. Ohara, "Growth of $Pb(Zr\text{-}Ti)O_3$ Single Crystal by Flux Method," Japan J. Appl. Phys., 7 953 (1968).

41. R. L. Cook and R. H. Dungan, "Hot Pressing of $PbZrO_3$-$PbTiO_3$ Ferroelectric Ceramics," Sandia Laboratory, Albuquerque, SCTM 240-263 [11] (1963).

42. J. J. Burke, N. L. Reed, and V. Weiss (editors), Ultrafine-Grain Ceramics, Chapter 8: T. Vasilos and W. Rhodes, "Fine Particulates to Ultrafine-Grain Ceramics," Sagamore Army Materials Research Conference, Syracuse Univ. Press, Syracuse, New York, pp. 137-171 (1970).

43. K. Zmbov, J. W. Hastie, and J. L. Margrave, "Mass Spectrometric Studies at High Temperatures. XXIV: Thermodynamics of Vaporization of SnF_2 and PbF_2 and the Dissociation Energies of SnF and PbF," Trans. Faraday Soc., 64 [4] 861-867 (1968).

44. R. H. Hauge, J. W. Hastie, and J. L. Margrave, "Ultraviolet Absorption Spectra of Gaseous SnF_2 and PbF_2," J. Phys. Chem., 72 [10] 3510-3511 (1968).

45. T. Ikeda, T. Oakno, and M. Watanabe, "A Ternary System PbO-TiO_2-ZrO_2," Japan J. Appl. Phys., 1 [4] 218 (1962).

46. A. H. Webster, R. C. MacDonald and W. S. Bowman, "The System PbO-ZrO_2 at 110°C," J. Can. Ceram. Soc., 34, 97-102 (1965).

47. J. L. Margrave (Ed.), The Characterization of High Temperature Vapors, Chapt. 6: R. C. Paule and J. L. Margrave, "Free-Evaporation and Effusion Techniques," pp. 130-151, John Wiley & Sons, Inc., New York (1967).

48. I. Langmuir, "The Vapor Pressure of Metallic Tungsten," Phys. Rev., 2 329-342 (1913).

49. W. D. Kingery (Ed.), Ceramic Fabrication Processes, Chapt. 15: J. E. Burke, "Recrystallization and Sintering in Ceramics," pp. 120-131, M.I.T. Press, Cambridge, Mass. (1963).

50. W. D. Kingery and B. Francois, "Grain Growth in Porous Compacts," J. Am. Ceram. Soc., 48 [10] 546-547 (1965).

51. W. P. Mason and H. Jaffe, "Methods for Measuring Piezoelectric, Elastic, and Dielectric Coefficients of Crystals and Ceramics," Proc. I.R.E., 42 921-930 (1954).

52. "IRE Standards on Piezoelectric Crystals: Measurement of Piezoelectric Ceramics, 1961," Proc. I.R.E., 49 1161-1169 (1961).

APPENDIX: Definitions and Relations of Ferroelectric and Piezoelectric Parameters

LIST OF SYMBOLS

Symbol	Definition	Unit
E_c	Coercive electric field	volt/centimeter
P_M	Maximum polarization	coulomb/centimeter^2
P_r	Remanent polarization	coulomb/centimeter^2
K	Dielectric constant	
d_p	Planar piezoelectric strain constant	meter/volt = coulomb/newton
d_{31}	Piezoelectric strain constant	meter/volt = coulomb/newton
g_{31}, g_p	Piezoelectric "voltage" constants	volt meter/newton = meter^2/coulomb
Δf	$f_a - f_r$	cycles/second = Hertz
f_a	Antiresonance frequency	cycles/second = Hertz
f_r	Resonance frequency	cycles/second = Hertz
k_{31}	Transverse coupling factor	
k_p	Planar coupling factor	
s_{11}	Elastic compliance constant	meter^2/newton
ϵ_{33}	Permittivity	farad/meter
C_s	Standard capacitor (1 mfd)	farad
q	Electric charge	coulomb
σ	Poisson ratio	
R_1	Root of a Bessel equation	
Veff	Effective voltage (rms)	volt

LIST OF SYMBOLS continued

Symbol	Definition	Unit
ρ	Density	grams/centimeter^3
A	Area	centimeter^2
d	Diameter of disk	centimeter
t	Thickness	centimeter
E(superscript)	At constant electric field	
D(superscript)	At constant electric displacement	
T(superscript)	At constant stress	

Relations

Ferroelectric:

$$E = Veff/t,\ P = q/A,\ q = C_s V$$

Piezoelectric: disk

$$k_p^2 = \frac{\Delta f}{f_r}\left[\frac{R_1 - (1-\sigma^2)}{1+\sigma}\right]\left[1 - \frac{\Delta f}{f_r}\left(\frac{R_1 - (1-\sigma^2)}{1+\sigma}\right)\right]$$

where $R_1 = 2.049$ for $\sigma = 0.3$.[51]

$$1/s_{11}^{E} = \frac{\pi^2 d^2 fr(1-\sigma)\rho}{R_1}$$

$$k_{31}^2 = k_p^2 \left(\frac{1-\sigma}{2}\right)$$

$$s_{11}^{D} = s_{11}^{E} \left(1-k_{31}^3\right)$$

$$d_{31}^2 = k_{31}^2 \left(\varepsilon_{33}^{T} s_{11}^{E}\right)$$

$$g_{31} = d_{31}/\varepsilon_{33}^{T}$$

$$g_p = dp/\varepsilon_{33}^{T}$$

The above relations were obtained from ref. 52.

TECHNICAL INFORMATION DIVISION
LAWRENCE BERKELEY LABORATORY
UNIVERSITY OF CALIFORNIA
BERKELEY, CALIFORNIA 94720